

AgentScore: Autoformulation of Deployable Clinical Scoring Systems

Silas Ruhrberg Estévez¹ Christopher Chiu¹ Mihaela van der Schaar¹

Abstract

Modern clinical practice relies on evidence-based guidelines implemented as compact scoring systems composed of a small number of interpretable decision rules. While machine-learning models achieve strong performance, many fail to translate into routine clinical use due to misalignment with workflow constraints such as memorability, auditability, and bedside execution. We argue that this gap arises not from insufficient predictive power, but from optimizing over model classes that are incompatible with guideline deployment. Deployable guidelines often take the form of unit-weighted clinical checklists, formed by thresholding the sum of binary rules, but learning such scores requires searching an exponentially large discrete space of possible rule sets. We introduce AgentScore, which performs semantically guided optimization in this space by using LLMs to propose candidate rules and a deterministic, data-grounded verification-and-selection loop to enforce statistical validity and deployability constraints. Across eight clinical prediction tasks, AgentScore outperforms existing score-generation methods and achieves AUC comparable to more flexible interpretable models despite operating under stronger structural constraints. On two additional externally validated tasks, AgentScore achieves higher discrimination than established guideline-based scores.

1. Introduction

Clinical decision-making is inherently difficult, requiring clinicians to act under uncertainty, time pressure, and incomplete information (Patton, 1978). Over recent decades, clinical guidelines have pushed medicine toward evidence-based care, moving beyond the opinions of individual clinicians (Sur & Dahm, 2011; Wieten, 2018). A central instrument in this shift is the clinical scoring system: a compact set of

¹DAMTP, University of Cambridge, Cambridge, UK. Correspondence to: Silas Ruhrberg Estevez <sr933@cam.ac.uk>.

Preprint. February 2, 2026.

explicit rules mapping a small number of routinely available patient measurements to risk strata or management recommendations (Challener et al., 2019). When well designed, such scores standardize decisions, support resource allocation, and facilitate communication across care settings (Woolf et al., 1999). From a machine learning perspective, these artifacts are best viewed not as approximate regressors, but as a deliberately constrained model family optimized for bedside execution, recall, and auditability (Ustun & Rudin, 2015).

Despite their ubiquity, effective scoring systems such as CURB-65 (Lim et al., 2003) must satisfy stringent practical requirements (Desai & Gross, 2019; Moons et al., 2015). They must rely on routinely available inputs, generalize across institutions despite missingness and measurement shift (Dambha-Miller et al., 2020), and remain interpretable and memorable for reliable bedside recall and audit without computational aids (Graham et al., 2011). Meeting these requirements in practice remains challenging. Most widely used scores are derived from expert consensus or manual analysis of observational studies (Woolf et al., 1999), often via regression models discretized for bedside use (see Fig. 1) (Sullivan et al., 2004). This process is labor-intensive, slow to update, and can yield brittle feature and threshold choices that are difficult to revise (Wasylewicz & Scheepers-Hoeks, 2018; Woolf et al., 1999).

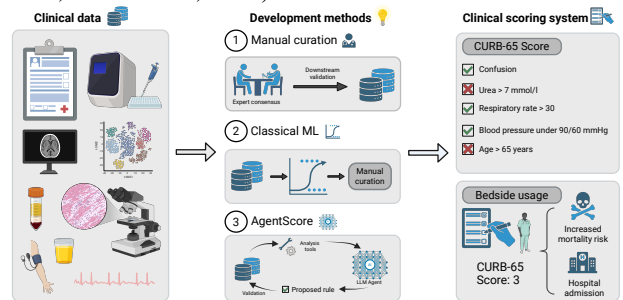


Figure 1. Clinical scoring systems: Guideline artifacts are compact, explicit checklists intended for reliable manual use.

In parallel, increasingly complex machine learning models have achieved strong performance on clinical prediction tasks (Takita et al., 2025; Killock, 2020; Shickel et al., 2018). However, even when accurate and ostensibly interpretable, many such models remain poorly matched to guideline deployment: they rely on inputs that are inconsistently available, require preprocessing and software-mediated in-

ference, and produce continuous-weight computations or decision thresholds that are difficult to execute and audit reliably at the bedside (Topol, 2019; Chen et al., 2021). This misalignment is reinforced by optimization incentives. Unconstrained models admit smooth parameterizations and efficient gradient-based training, whereas enforcing checklist structure induces a discrete subset selection problem with hard constraints on size and rule form, yielding a non-convex and often NP-hard objective (Ustun & Rudin, 2015; Bertsimas & Stellato, 2020). As a result, much of modern clinical ML implicitly optimizes over model classes that are convenient to train but incompatible with guideline workflows (Shortliffe & Sepulveda, 2018), while simple scores integrate directly into clinical practice (Graham et al., 2011).

Gap. Current clinical ML pipelines often treat deployability as a downstream engineering consideration rather than a first-class modeling constraint (Kelly et al., 2019). While recent work emphasizes *interpretability*, **interpretability does not guarantee deployability** (Lipton, 2018): a decision tree or sparse logistic regression may be human-understandable, but in its native form it typically cannot be executed and audited reliably at the bedside (e.g., floating-point arithmetic, non-memorable thresholds). Conversely, existing integer- and point-score learning methods largely optimize over a fixed, static feature matrix, and therefore lack a mechanism to systematically *construct* and search over derived guideline-style rules (e.g., temporal trends or physiologic ratios) that can materially improve checklist performance. A gap therefore remains for methods that jointly optimize *rule construction* and *checklist-compatibility constraints* by design.

Contributions

Conceptual. We formalize deployable clinical scoring systems as a constrained model class defined by unit-weighted checklists and a clinically motivated rule language supporting temporal patterns, physiologic ratios, and shallow compositions, explicitly encoding cognitive and operational constraints of bedside decision-making.

Algorithmic. We introduce AgentScore, a framework that bridges LLMs and discrete optimization: LLMs navigate the combinatorial space of semantic rule proposals, while a deterministic, data-grounded verification loop enforces statistical validity and sparsity.

Empirical. Across eight clinical prediction tasks spanning MIMIC-IV and eICU, AgentScore matches or exceeds state-of-the-art score-learning baselines under stricter structural constraints, and on two externally validated tasks it achieves higher discrimination than established guideline-based scores while remaining suitable for manual execution.

2. Deployable Clinical Scoring Systems

We treat bedside deployability as a hard modeling primitive rather than an auxiliary constraint. Accordingly, we restrict the hypothesis class itself to scoring systems that are natively compatible with clinical guidelines and routine bedside execution. Under this view, a clinical score is not an approximation to a continuous predictor, but a discrete decision object: a sparse, unit-weighted collection of human interpretable binary rules. Its structure is dictated by operational and cognitive constraints, including memorability, auditability, and arithmetic-free use, rather than by predictive expressiveness alone.

Problem setting. Let $\mathcal{D} = \{(\mathbf{X}_i, y_i)\}_{i=1}^N$ denote a dataset of patient trajectories, where $\mathbf{X}_i \in \mathbb{R}^{p \times T_i}$ is a matrix of p clinical variables observed over T_i timepoints for patient i , and $y_i \in \{0, 1\}$ is a binary outcome associated with each trajectory. For deployment, we compute a fixed, deployable representation $\tilde{\mathbf{x}}_i = \phi(\mathbf{X}_i) \in \mathbb{R}^{p'}$ that includes both static summaries and predefined temporal transformations; rules operate on $\tilde{\mathbf{x}}_i$.

Rule-based feature construction. A *rule* is a binary-valued predicate $r(\tilde{\mathbf{x}}) : \mathbb{R}^{p'} \rightarrow \{0, 1\}$, corresponding to a clinical statement, drawn from a restricted, clinically motivated rule language. The candidate rule dictionary is $\mathcal{R} = \{r_j(\tilde{\mathbf{x}})\}_{j=1}^{|\mathcal{R}|}$. The clinical checklists and the allowed rule families reflect constructs recurring in guideline-based scoring systems and bedside decision rules (see Appendix A).

Why unit-weighted checklists? Clinical scoring systems are typically applied under time pressure, interruption, and incomplete information, where cognitive load and memorability are primary bottlenecks (Miller, 1956). Empirically, widely adopted clinical guidelines almost universally take the form of short additive checklists composed of binary conditions and small total score ranges. Classical results on *improper linear models* further show that equal-weighted additive models often perform comparably to optimally weighted linear predictors (Dawes, 1979), aligning with evidence that simple, transparent heuristics are particularly effective under time pressure and uncertainty (Gigerenzer & Gaissmaier, 2011). Allowing non-unit weights increases mental arithmetic burden and reduces transparency, often necessitating calculators or electronic support. Similarly, deeply nested logic trees require tracking multiple contingent branches and intermediate states, which exceeds cognitive limits in bedside settings; as a result, such models are rarely adopted without computational mediation. We therefore adopt simplicity as an explicit design objective rather than a byproduct of regularization. By deliberately restricting the model class to the simplest structure, unit weighted N -of- M checklists, we maximize memorability, auditability, and reliable bedside execution.

Rule Language for Deployable Scoring Systems

(i) Numeric threshold rules.

$$r(\tilde{\mathbf{x}}) = \mathbb{I}[\tilde{x}_k \odot c], \quad \odot \in \{>, \geq, <, \leq\}, \quad c \in \mathbb{R}.$$

(ii) Numeric range rules.

$$r(\tilde{\mathbf{x}}) = \mathbb{I}[c_{\text{low}} \leq \tilde{x}_k \leq c_{\text{high}}].$$

(iii) Categorical inclusion rules.

$$r(\tilde{\mathbf{x}}) = \mathbb{I}[\tilde{x}_k \in \mathcal{A}].$$

(iv) Binary presence rules.

$$r(\tilde{\mathbf{x}}) = \mathbb{I}[\tilde{x}_k = 1].$$

(v) Physiological ratio and contrast rules.

$$r(\tilde{\mathbf{x}}) = \mathbb{I}[g(\tilde{\mathbf{x}}) \odot c], \quad g(\tilde{\mathbf{x}}) \in \left\{ \frac{\tilde{x}_a}{\tilde{x}_b}, \tilde{x}_a - \tilde{x}_b \right\},$$

(vi) Count-based rules.

$$r(\tilde{\mathbf{x}}) = \mathbb{I}\left[\sum_{j \in \mathcal{J}} r_j(\tilde{\mathbf{x}}) \geq m'\right].$$

(vii) Logical composition rules. Given base rules $r_{\ell=1}^L$, we allow shallow Boolean compositions (AND/OR). We define $\text{Depth}(r)$ as the number of logical operations and restrict it to preserve bedside memorability:

$$r(\tilde{\mathbf{x}}) = \begin{cases} \bigwedge_{\ell=1}^L r_{\ell}(\tilde{\mathbf{x}}) & (\text{AND}), \\ \bigvee_{\ell=1}^L r_{\ell}(\tilde{\mathbf{x}}) & (\text{OR}). \end{cases}$$

(viii) Temporal and distributional rules. Temporal rules operate on predefined summaries of longitudinal measurements included in $\tilde{\mathbf{x}}_i = \phi(\mathbf{X}_i)$: $r(\tilde{\mathbf{x}}_i) = \mathbb{I}[h(\mathbf{X}_i) \odot c]$.

$$h(\mathbf{X}_i) \in \left\{ \Delta x_k^{(t)}, \frac{x_k^{(t)} - x_k^{(0)}}{x_k^{(0)}}, \max_t x_k^{(t)} - \min_t x_k^{(t)} \right\},$$

In addition, we allow distributional normalizations, including quantile-based rules $\mathbb{I}[\tilde{x}_k \odot Q_k(q)]$, standardized rules $\mathbb{I}[(\tilde{x}_k - \mu_k)/\sigma_k \odot z]$, and percent-change rules $\mathbb{I}[\Delta x_k/x_k \odot \gamma]$.

Score definition. A clinical scoring system selects a subset $\mathcal{S} \subseteq \mathcal{R}$ of at most m rules and assigns each a unit weight: $S(\tilde{\mathbf{x}}) = \sum_{r_j \in \mathcal{S}} r_j(\tilde{\mathbf{x}})$, yielding a discrete score $S(\tilde{\mathbf{x}}) \in \{0, 1, \dots, m\}$. An integer threshold $\tau \in \{0, \dots, m\}$ induces a binary clinical decision rule:

$$\hat{y}(\tilde{\mathbf{x}}) = \begin{cases} 1, & S(\tilde{\mathbf{x}}) \geq \tau, \\ 0, & \text{otherwise.} \end{cases}$$

The resulting model is a unit-weighted N -of- M checklist, with $M = |\mathcal{S}|$ denoting the number of rules and $N = \tau$ the decision threshold. If a required feature \tilde{x}_k is missing at prediction time, the rule evaluates to false, ensuring conservative risk assessment.

Optimization objective. We seek guideline-style scoring systems that maximize empirical clinical utility under de-

ployability constraints:

$$\begin{aligned} \max_{\mathcal{S} \subseteq \mathcal{R}} \quad & \mathcal{U}(S(\tilde{\mathbf{x}}), y; \mathcal{D}_{\text{val}}) \\ \text{s.t.} \quad & |\mathcal{S}| \leq m, \quad \text{Depth}(r) \leq d \quad \forall r \in \mathcal{S}. \end{aligned} \quad (1)$$

Here \mathcal{U} denotes an empirical, non-convex utility (e.g., AUC, net benefit, or decision-curve utility) evaluated on held-out data. This optimization is NP-hard and non-differentiable due to discrete rule selection and combinatorial structural constraints (Ustun & Rudin, 2015). Unlike continuous relaxations or surrogate losses, we directly optimize the target utility via constrained, agent-guided search, ensuring that deployability constraints are enforced throughout.

Definition 2.1 (Deployable Clinical Scoring System). A *deployable clinical scoring system* is a tuple $\mathcal{G} = (\mathcal{S}, S, \tau)$, where $\mathcal{S} \subseteq \mathcal{R}$ is a finite set of binary, human-interpretable rules, $S(\tilde{\mathbf{x}}) = \sum_{r_j \in \mathcal{S}} r_j(\tilde{\mathbf{x}})$ is an integer-valued score, and τ is a decision threshold. The system is *deployable* if it satisfies:

- 1. Parsimony:** $|\mathcal{S}| \leq m$ for small m .
- 2. Interpretability:** Each rule corresponds to a clinically meaningful statement over routinely collected variables.
- 3. Memorability:** Rules are binary, unit-weighted, and shallowly composed, enabling reliable recall and manual application.
- 4. Operational deployability:** Evaluation requires no specialized computational infrastructure.
- 5. Predictive adequacy:** The model achieves acceptable discrimination and calibration on the target population, subject to the above constraints.

Example: UK CF Registry 1-year Mortality Score. AgentScore produces compact, guideline-style checklists. Table 1 shows one representative instantiation of a one-year mortality score. The resulting score instantiates multiple allowed rule families. Importantly, the listed rules are derived constructs rather than raw dataset columns; instead, they are constructed by AgentScore.

Table 1. UK CF Registry one-year mortality checklist generated by AgentScore. Each satisfied rule contributes one point.

Checklist rule (satisfied?)	Points
FEV ₁ predicted $\geq 15\%$ decline from 5-year best	+1
Current FEV ₁ predicted $\leq 50\%$	+1
Current FEV ₁ predicted $\leq 30\%$	+1
IV antibiotics: ≥ 15 days (hospital) or ≥ 20 days (home)	+1
High-risk threshold	S($\tilde{\mathbf{x}}$) ≥ 2

Table 2. Comparison of representative interpretable score-learning approaches. Prior methods optimize linear, additive, or sequential rule models over fixed feature encodings. In contrast, AgentScore targets deployable-by-design, unit-weighted checklist scores by searching a guideline-compatible rule language under hard structural constraints.

Method	Score form	Weights	Rule language	Search / construction	Derived rule construction	Unit-weighted unordered checklist
RiskSLIM	linear score	non-unit integers	binned thresholds / fixed binaries	MIP over coefficients	✗	✗
FasterRisk	linear score	non-unit integers	binned thresholds / fixed binaries	approximate integer optimization	✗	✗
AutoScore	additive score	non-negative integers	binned thresholds	pipeline (rank → bin → score)	✗	✗
CORELS	rule list	N/A (sequential logic)	binarized features / thresholds	branch-and-bound search	✗	✗
AgentScore	<i>N</i> -of- <i>M</i> checklist	unit (0/1)	clinical rules / thresholds	constrained search + validation	✓	✓

3. Related Works

Our work lies at the intersection of (i) interpretable machine learning, (ii) sparse clinical score learning, and (iii) LLM-guided rule generation. Extended comparisons are provided in Appendix C.

General interpretable models in healthcare. A broad class of methods targets predictive performance while maintaining transparency. Generalized additive models (GAMs) such as Explainable Boosting Machines (EBMs) (Hastie & Tibshirani, 1986; Nori et al., 2019) and sparse linear models (e.g., LASSO) provide intelligibility via shape functions or feature selection, and are often used as pragmatic baselines on tabular clinical data. However, *interpretability* alone does not ensure reliable, unaided bedside deployment (Lipton, 2018). These models typically yield continuous coefficients (e.g., $0.41 \times \text{Age}$), require non-trivial arithmetic, or rely on look-up tables for non-linear terms, making unaided manual use difficult at the point of care. Moreover, they do not typically enforce the operational constraints of guideline artifacts, such as bounded score ranges, unit weights, and unordered checklist execution. Rule-based models such as **CORELS** (Angelino et al., 2018), optimal decision trees including **GOSDT** (Hu et al., 2019), and **Bayesian Rule Lists** (Letham et al., 2015) offer alternative forms of interpretability. However, these models rely on ordered or hierarchical evaluation, in contrast to the unordered, additive checklist structure typical of clinical scoring systems. We also include heuristic scoring pipelines such as **AutoScore** (Xie et al., 2020). While **AutoScore** produces integer-valued point systems, it often produces multi-bin point systems with wider score ranges and non-unit weights, which can increase cognitive load compared with short unit-weighted checklists (Graham et al., 2011).

Sparse clinical score learning. Distinct from general interpretable ML, score-learning methods explicitly construct compact points-based scores intended for manual execution. Integer-weighted methods such as **RiskSLIM** (Ustun & Rudin, 2015) and **FasterRisk** (Liu et al., 2022) formulate learning as integer optimization over sparse models with small integer coefficients, producing concise linear point systems with strong face validity. This line complements classical regression-to-points pipelines that discretize and round coefficients to obtain integer scores, but still typi-

cally retain non-unit weights and arithmetic burden. However, even short scores can remain operationally challenging when they use non-unit or signed weights (e.g., $+5, -3$), increasing mental arithmetic burden and error risk under time pressure. More importantly, these methods typically optimize over a fixed feature matrix: they can select among pre-computed columns, but do not systematically construct new semantic rules such as physiologic ratios, temporal changes, percentile-based thresholds, or logical compositions unless these are manually engineered *a priori*. Consequently, semantic feature engineering and rule design remain manual prerequisites, limiting coverage of the combinatorial rule space that clinical guideline authors routinely explore. In contrast to points-based coefficient learning, our target object is an unordered clinical checklist with unit weights, where the primary challenge is discovering and validating the rules themselves rather than optimizing coefficients.

LLM-guided rule and feature generation. Large language models have been explored for structured discovery, including feature generation, program synthesis, and guidance in combinatorial search spaces (Nam et al., 2024; Balek et al., 2025; Liu et al., 2025). In clinical settings, prior work reports limitations in robustness, calibration, and guideline adherence when LLMs are used as standalone decision-makers (Williams et al., 2024; Artsi et al., 2025). We instead constrain LLMs to a narrow, verifiable role: proposing candidate rules within a restricted, guideline-compatible language that encodes admissible rule families and shallow compositions. All proposals are subsequently screened and selected using held-out patient data under explicit deployability constraints (unit weights, bounded size, limited depth), so LLMs act as semantic proposal mechanisms embedded in a deterministic, data-grounded optimization loop rather than as autonomous decision-makers. This separation of semantic proposal from statistical verification yields reproducible rule selection and ensures that every retained rule is both interpretable and empirically supported. As longitudinal EHR signals become increasingly available, the bottleneck shifts from data scarcity to synthesizing deployable rules from routine measurements; we address this by combining LLM-guided proposal over a guideline-compatible rule language with deterministic, data-grounded validation under hard checklist constraints.

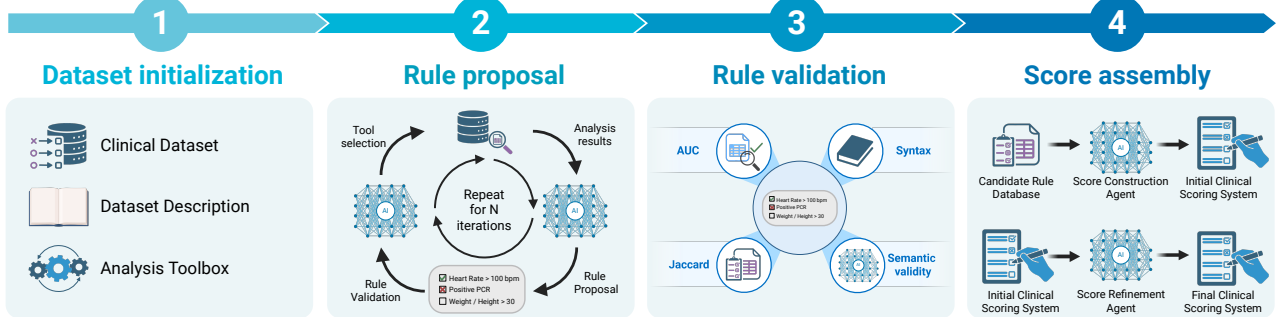


Figure 2. Overview of AgentScore. An LLM-based proposal agent generates candidate rules from a dataset description and tool-mediated aggregate statistics; it never receives patient-level records. Proposed rules are screened by a deterministic validation module enforcing statistical performance and grammar-level deployability constraints (e.g., complexity limits, unit weights). Statistically admissible rules are reviewed by a clinical plausibility agent to filter semantically incoherent proposals, after which a score assembly agent selects a compact clinical checklist from the retained pool and the evaluation tools choose the operating threshold.

4. AgentScore

Problem setup. Learning deployable clinical scoring systems imposes three competing requirements. First, candidate rules must express clinically meaningful semantics, including derived quantities, temporal patterns, and shallow compositional constructs that are rarely available as explicit features in clinical datasets. Second, rule generation must be strictly data-grounded and robust to hallucination, bias, and spurious correlations, with every decision evaluated under explicit, verifiable metrics. Third, the resulting scores must satisfy hard deployability constraints while retaining acceptable predictive utility. Formally, we seek to learn a unit-weighted checklist rule set $\mathcal{S} = \{r_1, \dots, r_{|\mathcal{S}|}\} \subseteq \mathcal{R}$ from a structured rule space \mathcal{R} that maximizes predictive utility $\mathcal{U}(\mathcal{S})$ subject to hard constraints on rule structure and checklist size, i.e., $|\mathcal{S}| \leq m$. This induces a constrained subset selection problem over \mathcal{R} that is NP-hard, rendering exhaustive or purely optimization-based approaches intractable at the required level of expressiveness. This intractability is driven by the combinatorial growth of the rule space under even modest grammars and depth limits (see Appendix E).

LLM usage: proposal vs. verification. Injecting semantic understanding and domain knowledge into rule construction naturally motivates the use of LLMs. However, direct and unconstrained application of LLMs is unsuitable in medical settings: free-form generation provides no guarantees of validity or empirical grounding and introduces significant hallucination risks. Conversely, existing score-learning pipelines operating over fixed feature encodings are limited to pre-specified thresholds and binned variables, and cannot systematically discover higher-level clinical rules without exponential enumeration or extensive manual feature engineering. We therefore introduce AgentScore, a framework that treats LLMs not as a decision-maker, but as a *structured semantic proposal mechanism* embedded within a deterministic, tool-mediated evaluation loop. This design enables tractable search over an expressive, guideline-compatible hypothesis class while enforcing data grounding

via tool verification and deployability by construction. Algorithmically, AgentScore instantiates an LLM-assisted combinatorial optimization procedure in which semantic exploration is decoupled from acceptance and optimization, yielding auditable, data-driven rule induction.

Overview. AgentScore approximates the resulting checklist learning problem via a decomposition into three stages: *rule proposal*, *rule filtering*, and *score assembly* (Figure 2). Each stage enforces a disjoint subset of constraints, enabling tractable optimization over the guideline-compatible rule space. Complete algorithmic specifications, including pseudocode, tool interfaces, and prompts, are provided in Appendix F and Appendix G.

Rule proposal. Candidate rules are proposed by a language-model agent constrained to emit structured rules from a pre-defined grammar (Appendix A). The agent does not observe patient-level data and interacts with the dataset exclusively through a fixed tool interface exposing feature metadata and aggregate evaluation statistics. Proposals are generated in small batches per iteration to control exploration of the combinatorial rule space.

Deterministic validation module. Each proposed rule is deterministically evaluated using the tool interface. The validation module enforces both statistical performance and grammar-level deployability constraints. A rule r is retained only if it satisfies a minimum discrimination threshold τ_{rule} and passes redundancy checks with respect to previously retained rules:

$$\text{AUROC}(r) \geq \tau_{\text{rule}}, \quad \max_{r' \in \mathcal{P}} J^+(r, r') \leq \delta,$$

where \mathcal{P} denotes the current pool of retained rules, and J^+ denotes Jaccard similarity computed over positive-class coverage vectors on \mathcal{D}_{val} . Rules failing either criterion are discarded without further consideration. We set τ_{rule} deliberately low: because checklists are compact and each rule increases cognitive burden, we require every retained rule to be individually meaningful while allowing checklist-level evaluation to select complementary weak signals.

Clinical plausibility agent. All rules passing deterministic validation are subsequently reviewed by a clinical plausibility agent, an independent LLM-based self-check. This agent evaluates whether a rule corresponds to a coherent and defensible clinical statement given the variable semantics and transformations used. Rules judged implausible or clinically nonsensical are rejected *prior to final retention*, ensuring that only rules satisfying both statistical and semantic criteria enter the candidate pool. Importantly, this filter is purely eliminative: it does not propose, modify, or rank rules, and cannot introduce new structure into the score.

Score construction agent. Given the retained pool \mathcal{P} , a third agent proposes a checklist $\mathcal{S} \subseteq \mathcal{P}$ with $|\mathcal{S}| \leq m$. We employ an agent for this step rather than an exact solver (e.g., MIP) to encourage semantic diversity. While exact solvers maximize statistical utility, they can select highly correlated proxies for the same underlying signal (e.g., multiple variants of blood pressure). The agent can construct checklists that cover distinct physiological domains (e.g., respiratory, cardiovascular, renal), aligning the final score with clinical reasoning principles for robust multi-organ assessment. Each proposed checklist is evaluated deterministically via the tool interface to yield discrimination and coverage metrics. Across proposals and refinement steps, we retain the best-performing checklist on \mathcal{D}_{val} under the target utility \mathcal{U} , ensuring that semantic guidance affects which subsets are explored but not how the final checklist is selected.

Iterative refinement. The score construction agent may iteratively refine its proposal over a fixed number of steps, receiving updated evaluation metrics after each revision. Refinement operations are limited to rule inclusion or exclusion within the retained pool \mathcal{P} . Importantly, the decision threshold τ defining the positive class (i.e., $S(\bar{\mathbf{x}}) \geq \tau$) is optimized automatically by the evaluation tools by maximizing Youden’s J statistic on validation data and is *not* selected by the agent.

5. Experiments

We evaluate the clinical scoring systems learned by AgentScore across a diverse set of real-world clinical prediction tasks. Our evaluation is structured around four questions:

- (i) **Predictive adequacy:** Can deployable, unit-weighted checklists learned by AgentScore achieve discrimination comparable to interpretable but less deployable machine learning models?
- (ii) **Guideline competitiveness:** How do the learned scores compare to established clinical guidelines under realistic cross-institutional evaluation?
- (iii) **Practical deployability:** Do the resulting scoring sys-

tems satisfy the cognitive and operational constraints required for bedside use?

- (iv) **Ablation study:** Why is iterative, multi-step agent-based search necessary to achieve effective performance under these constraints?

Unless otherwise stated, all main experiments use GPT-5 as the agent backbone. Additional analyses of the learned guidelines and comparisons across different LLM backbones are provided in Appendix E.

5.1. Predictive Performance

Datasets and Tasks. We evaluate AgentScore on eight real-world clinical prediction tasks derived from the publicly available MIMIC-IV and eICU EHR datasets, spanning mortality, length-of-stay, and clinically actionable intervention prediction. All tasks use only variables routinely available at the time of clinical decision-making. We perform 5-fold cross-validation, holding out 20% of patients in each fold as a test set used exclusively for final evaluation. Reported metrics are computed on held-out test splits and aggregated across folds. For AgentScore, we further split the training portion, using 20% of the training patients as validation. Additional details are provided in Appendix D.

Baselines. We compare AgentScore against a comprehensive set of interpretable and score-learning approaches representing strong alternatives for clinical risk prediction under varying degrees of structural constraint. These include state-of-the-art integer-valued scoring methods such as RiskSLIM and FasterRisk, as well as pooled penalized logistic regression (PLR) baselines (Liu et al., 2022). While these methods produce compact and interpretable models, they do not enforce unit weighting, checklist-style execution, or bounded logical complexity during learning. As interpretable upper bounds, we additionally evaluate logistic regression, decision trees, and the AutoScore framework. These models often achieve strong discrimination but rely on flexible coefficients and inference pipelines that violate guideline-style deployability constraints.

Results. Among score-generation baselines that learn small integer-weighted scores (RiskSLIM, FasterRisk, and PLR variants), AgentScore is competitive and improves over these integer-score methods despite operating under stricter checklist-deployability constraints. We include pooled PLR baselines primarily to illustrate the brittleness of post-hoc coefficient modification in logistic models (e.g., threshold pooling and rounding), which can substantially degrade discrimination; by contrast, RiskSLIM and FasterRisk mitigate this brittleness via dedicated integer optimization over coefficients.

We additionally report logistic regression, decision trees, and the AutoScore pipeline. These methods can achieve

Table 3. Model performances. AgentScore enforces unit weights, bounded size, and checklist structure, while competing methods do not. Entries are mean \pm std. For each dataset, the best-performing score-based method (highest mean AUROC) is shown in **bold**.

Method	MIMIC AF	MIMIC COPD	MIMIC HF	MIMIC AKI	MIMIC Cancer	MIMIC Lung	eICU LOS	eICU Vaso	Mean
Decision Tree	0.79 \pm 0.01	0.69 \pm 0.01	0.77 \pm 0.02	0.85 \pm 0.00	0.64 \pm 0.01	0.66 \pm 0.00	0.69 \pm 0.00	0.77 \pm 0.00	0.73 \pm 0.07
Logistic (L1)	0.77 \pm 0.01	0.68 \pm 0.01	0.76 \pm 0.01	0.78 \pm 0.00	0.64 \pm 0.02	0.65 \pm 0.01	0.69 \pm 0.00	0.75 \pm 0.00	0.72 \pm 0.05
AutoScore	0.82 \pm 0.00	0.66 \pm 0.01	0.81 \pm 0.01	0.84 \pm 0.00	0.60 \pm 0.01	0.66 \pm 0.00	0.63 \pm 0.00	0.75 \pm 0.00	0.72 \pm 0.09
FasterRisk	0.75 \pm 0.02	0.62 \pm 0.00	0.73 \pm 0.01	0.76 \pm 0.00	0.57 \pm 0.01	0.54 \pm 0.00	0.70 \pm 0.00	0.75 \pm 0.00	0.68 \pm 0.08
RiskSLIM	0.75 \pm 0.01	0.62 \pm 0.00	0.74 \pm 0.01	0.80 \pm 0.00	0.58 \pm 0.01	0.56 \pm 0.03	0.62 \pm 0.00	0.64 \pm 0.01	0.66 \pm 0.08
Pooled PLR (RDU)	0.70 \pm 0.01	0.58 \pm 0.00	0.73 \pm 0.03	0.73 \pm 0.00	0.55 \pm 0.01	0.61 \pm 0.01	0.67 \pm 0.00	0.64 \pm 0.00	0.65 \pm 0.06
Pooled PLR (RSRD)	0.70 \pm 0.01	0.58 \pm 0.00	0.70 \pm 0.01	0.76 \pm 0.00	0.55 \pm 0.01	0.59 \pm 0.02	0.62 \pm 0.00	0.64 \pm 0.00	0.64 \pm 0.07
Pooled PLR (Rand)	0.70 \pm 0.01	0.58 \pm 0.00	0.70 \pm 0.01	0.76 \pm 0.00	0.55 \pm 0.01	0.50 \pm 0.00	0.62 \pm 0.00	0.50 \pm 0.00	0.62 \pm 0.09
Pooled PLR (RDP)	0.70 \pm 0.01	0.58 \pm 0.00	0.70 \pm 0.01	0.76 \pm 0.00	0.55 \pm 0.01	0.50 \pm 0.00	0.62 \pm 0.00	0.50 \pm 0.00	0.62 \pm 0.09
Pooled PLR (RDSP)	0.70 \pm 0.01	0.58 \pm 0.00	0.70 \pm 0.01	0.76 \pm 0.00	0.55 \pm 0.01	0.50 \pm 0.00	0.62 \pm 0.00	0.50 \pm 0.00	0.62 \pm 0.09
Pooled PLR (RD)	0.70 \pm 0.01	0.58 \pm 0.00	0.70 \pm 0.01	0.76 \pm 0.00	0.55 \pm 0.01	0.50 \pm 0.00	0.62 \pm 0.00	0.50 \pm 0.00	0.60 \pm 0.10
AgentScore	0.81 \pm 0.01	0.63 \pm 0.03	0.79 \pm 0.01	0.79 \pm 0.02	0.59 \pm 0.01	0.63 \pm 0.00	0.67 \pm 0.00	0.76 \pm 0.00	0.71 \pm 0.08

higher AUROC, but they are not checklist-deployable by design: they rely on learned (non-unit) integer coefficients, post-hoc discretization, or model execution requirements that impose arithmetic and operational overhead relative to unit-weighted clinical checklists.

Averaged across all eight tasks, AgentScore significantly improves AUROC over integer score-learning baselines, with mean fold-level gains of +0.046 vs. RiskSLIM and +0.031 vs. FasterRisk. Two-sided paired tests on fold-level AUROCs ($n = 40$; Holm–Bonferroni corrected) reject equality for all score-based baselines ($p < 0.001$). Full results are included in Appendix E.

5.2. Guideline Competitiveness

In the previous section, we compared AgentScore against strong interpretable machine-learning baselines that do not satisfy guideline-style deployability constraints. We now evaluate a different and clinically relevant question: whether data-driven, deployable scoring systems learned by AgentScore can compete with *established clinical guidelines* under out-of-distribution evaluation settings that mimic the validation procedures used prior to clinical deployment.

Evaluation protocol. We evaluate guideline competitiveness under a cross-institutional setting. AgentScore is trained on data from one institution and evaluated on an independent external cohort. For fairness, existing clinical guidelines are applied without modification to their rule structure; only the decision threshold is calibrated on the same training data used for AgentScore, isolating the quality of the underlying rule sets rather than threshold selection.

Results. Using a PhysioNet ICU 2012 mortality benchmark, we compare AgentScore against the SOFA (Vincent et al., 1996) and SAPS-I scores (Gall et al., 1984), two widely used ICU risk stratification tools. To further assess robustness across healthcare systems and disease domains, we train AgentScore on a UK cystic fibrosis cohort and evaluate performance on an independent Canadian cohort.

We compare against commonly used lung-transplantation eligibility guidelines for identifying high-risk individuals (Ramos et al., 2019) and a simple, widely used FEV₁-based threshold (FEV₁ < 30%) (Ramos et al., 2017). Figure 3 shows that AgentScore achieves higher discrimination than the established guidelines under external validation.

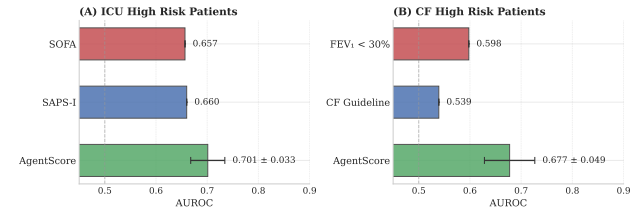


Figure 3. External validation against guidelines. AgentScore outperforms clinical guidelines in AUROC (mean \pm std over 5 seeds; guidelines deterministic).

5.3. Practical Deployability

We conducted a structured expert review of score deployability with a panel of $N = 18$ practicing clinicians (89% with ≥ 6 years of clinical experience) from six countries. Participants evaluated four representative AgentScore checklists alongside matched outputs from FasterRisk and participants were instructed to assume equal predictive performance. Across 72 pairwise judgments per question, participants significantly preferred AgentScore-generated checklists for alignment with guideline-style reasoning (85% vs. 15%; binomial $p < 10^{-9}$, Cohen's $h = 0.77$), ease of bedside application (71% vs. 29%; $p < 10^{-3}$, $h = 0.43$), and deployment preference (81% vs. 19%; $p < 10^{-7}$, $h = 0.66$). For overall model preference, 67% of clinicians selected AgentScore, 6% selected FasterRisk, and 28% reported no preference ($\chi^2(2) = 10.3$, $p = 0.006$). Full methodology, question wording, and per-question response distributions are provided in Appendix E.6.

5.4. Ablation Studies

We conduct targeted ablation studies to isolate the contribution of key components of AgentScore (see Table 4). In the *LLM Only* ablation, we replace the constrained proposal–evaluation loop with a single unconstrained language model,

removing tool-mediated validation and iterative feedback. In the *Single-Pass* ablation, we disable iterative refinement while retaining full evaluation tools. We further ablate structural constraints. The *No Jaccard* variant disables redundancy filtering based on positive-class Jaccard overlap, allowing highly overlapping rules to co-exist. The *No Diversity* variant disables rule-type diversity enforcement that encourages diverse rule family sampling.

Table 4. Ablation study of AgentScore components. Mean AUROC is averaged across datasets, with standard deviation computed across tasks.

Ablation	Mean AUROC	Std
Full AgentScore	0.71	0.08
LLM Only (unconstrained)	0.59	0.07
Single-Pass (no refinement)	0.69	0.07
No Jaccard	0.69	0.08
No Rule Diversity	0.70	0.08

6. Discussion

Despite high predictive accuracy in retrospective evaluations, many clinical machine-learning models fail to translate into real-world impact. A central reason is persistent misalignment with clinical workflows: complex models often depend on dense or non-routinely available inputs, specialized computational infrastructure, and opaque inference procedures. These barriers are particularly pronounced in resource-constrained settings.

In this work, we argue that meaningful clinical impact does not always require increasingly large or expressive models. Instead, it requires leveraging machine learning to *improve existing clinical workflows* while respecting the structural, cognitive, and operational constraints under which medical decisions are made. From this perspective, clinical scoring systems are not a legacy artifact to be replaced, but a deliberately constrained hypothesis class optimized for deployment.

We introduce AgentScore, a constrained learning framework that automatically constructs unit-weighted clinical checklists under explicit deployability constraints. Computational resources are required only during development; deployment reduces to evaluating a small set of binary rules and summing their outputs, enabling bedside use without calculators, servers, or continuous model maintenance. Beyond deployability, AgentScore addresses a key barrier to clinical ML adoption: data governance. Rule generation is mediated through a restricted tool interface and decoupled from direct data access. Large language models never observe raw patient records and interact only through a restricted tool interface that returns aggregate statistics. This can simplify governance and audit in collaborations where direct access to patient-level data is limited, although aggregate interfaces still require careful privacy controls.

More broadly, our results suggest that much of the predictive signal exploited by flexible interpretable models can be retained within a tightly constrained, deployable hypothesis class when semantic rule construction, deterministic evaluation, and structured selection are jointly enforced. This challenges the common implicit assumption that clinical machine learning must trade deployability for performance, and highlights constrained optimization over guideline-compatible model classes as a promising direction for future research.

Limitations. Clinical scoring systems necessarily trade expressivity for simplicity. While such systems can standardize care and improve outcomes at the population level, they cannot capture all nuances of individual patient trajectories, and clinical judgment remains essential. Since AgentScore is less expressive than flexible statistical or black-box models, it is not expected to consistently outperform them in raw predictive performance. Rule discovery is also *knowledge-bounded*: although acceptance is data-grounded via deterministic evaluation, the candidate rules are mediated by the LLM and limited by the constructs it can surface; thus, predictive relationships may be missed if they are not semantically accessible to the agent. Furthermore, AgentScore prioritizes semantic meaningfulness and deployability over formal optimization guarantees and does not guarantee convergence to a globally optimal checklist, which is generally intractable for this problem class anyway. While our framework enforces deployability constraints, it does not explicitly enforce fairness constraints across demographic subgroups. Like all data-driven methods, AgentScore may learn rules that reflect historical biases in clinical practice or documentation patterns; formal fairness auditing and subgroup validation remain essential prior to deployment. Finally, while our framework reduces reliance on direct data access during learning, it does not eliminate the need for careful dataset curation and does not by itself guarantee robustness under distribution shift.

Conclusion and clinical perspective. AgentScore demonstrates that machine learning can be used not to replace clinical guidelines, but to *systematically improve them*. By learning compact, interpretable, and auditable unit-weighted checklists that align with real clinical workflows, our approach provides a pathway to generate candidate scoring systems for prospective validation. More broadly, AgentScore exemplifies a framework for constrained semantic optimization, in which hypothesis class design, deployability, and verification are treated as first-class modeling concerns. Similar additive checklist structures already appear in other safety-critical settings, including aviation safety checklists (e.g., pre-flight procedures) and financial lending decisions (e.g., credit scoring), suggesting broader applicability beyond healthcare.

Impact statement

This paper presents work whose goal is to advance the field of machine learning by proposing a framework for constructing interpretable checklist models under explicit deployability constraints. The scoring systems produced in this paper are research artifacts only and are not intended for clinical use. As with any model trained on observational data, they may reflect bias or dataset artifacts and could cause harm if deployed without expert review, external validation, and regulatory oversight. Our aim is to contribute a methodological perspective on clinically aligned model design, not to promote real-world deployment.

References

Adebayo, J., Gilmer, J., Muelly, M., Goodfellow, I., Hardt, M., and Kim, B. Sanity checks for saliency maps. In *Proceedings of the 32nd International Conference on Neural Information Processing Systems*, NIPS'18, pp. 9525–9536, Red Hook, NY, USA, 2018. Curran Associates Inc.

Angelino, E., Larus-Stone, N., Alabi, D., Seltzer, M., and Rudin, C. Learning certifiably optimal rule lists for categorical data. *Journal of Machine Learning Research*, 18(234):1–78, 2018. URL <http://jmlr.org/papers/v18/17-716.html>.

Artsi, Y., Sorin, V., Glicksberg, B. S., Korfiatis, P., Freeman, R., Nadkarni, G. N., and Klang, E. Challenges of implementing llms in clinical practice: Perspectives. *Journal of Clinical Medicine*, 14(17):6169, September 2025. ISSN 2077-0383. doi: 10.3390/jcm14176169. URL <http://dx.doi.org/10.3390/jcm14176169>.

Balek, V., Sýkora, L., Sklenák, V., and Kliegr, T. Llm-based feature generation from text for interpretable machine learning. *Machine Learning*, 114(11), October 2025. ISSN 1573-0565. doi: 10.1007/s10994-025-06867-1. URL <http://dx.doi.org/10.1007/s10994-025-06867-1>.

Bellomo, R., Ronco, C., Kellum, J. A., Mehta, R. L., and Palevsky, P. Acute renal failure – definition, outcome measures, animal models, fluid therapy and information technology needs: the second international consensus conference of the acute dialysis quality initiative (adqi) group. *Critical Care*, 8(4), May 2004. ISSN 1364-8535. doi: 10.1186/cc2872. URL <http://dx.doi.org/10.1186/cc2872>.

Bertsimas, D. and Stellato, B. The voice of optimization. *Machine Learning*, 110(2):249–277, July 2020. ISSN 1573-0565. doi: 10.1007/s10994-020-05893-5. URL <http://dx.doi.org/10.1007/s10994-020-05893-5>.

Bishop, E. H. Pelvic scoring for elective induction. *Obstetrics & Gynecology*, 24:266–268, 1964.

Blatchford, O., Murray, W. R., and Blatchford, M. A risk score to predict need for treatment for uppergastrointestinal haemorrhage. *The Lancet*, 356(9238):1318–1321, October 2000. ISSN 0140-6736. doi: 10.1016/s0140-6736(00)02816-6. URL [http://dx.doi.org/10.1016/S0140-6736\(00\)02816-6](http://dx.doi.org/10.1016/S0140-6736(00)02816-6).

Bone, R. C., Balk, R. A., Cerra, F. B., Dellinger, R. P., Fein, A. M., Knaus, W. A., Schein, R. M., and Sibbald, W. J. Definitions for sepsis and organ failure and guidelines for the use of innovative therapies in sepsis. *Chest*, 101(6):1644–1655, June 1992. ISSN 0012-3692. doi: 10.1378/chest.101.6.1644. URL <http://dx.doi.org/10.1378/chest.101.6.1644>.

Brunton, S. L., Proctor, J. L., and Kutz, J. N. Discovering governing equations from data by sparse identification of nonlinear dynamical systems. *Proceedings of the National Academy of Sciences*, 113(15):3932–3937, March 2016. ISSN 1091-6490. doi: 10.1073/pnas.1517384113. URL <http://dx.doi.org/10.1073/pnas.1517384113>.

Cao, K., Xia, Y., Yao, J., Han, X., Lambert, L., Zhang, T., Tang, W., Jin, G., Jiang, H., Fang, X., Nogues, I., Li, X., Guo, W., Wang, Y., Fang, W., Qiu, M., Hou, Y., Kovarnik, T., Vocka, M., Lu, Y., Chen, Y., Chen, X., Liu, Z., Zhou, J., Xie, C., Zhang, R., Lu, H., Hager, G. D., Yuille, A. L., Lu, L., Shao, C., Shi, Y., Zhang, Q., Liang, T., Zhang, L., and Lu, J. Large-scale pancreatic cancer detection via non-contrast ct and deep learning. *Nature Medicine*, 29(12):3033–3043, November 2023. ISSN 1546-170X. doi: 10.1038/s41591-023-02640-w. URL <http://dx.doi.org/10.1038/s41591-023-02640-w>.

Centor, R. M., Witherspoon, J. M., Dalton, H. P., Brody, C. E., and Link, K. The diagnosis of strep throat in adults in the emergency room. *Medical Decision Making*, 1(3):239–246, August 1981. ISSN 1552-681X. doi: 10.1177/0272989x8100100304. URL <http://dx.doi.org/10.1177/0272989x8100100304>.

Challener, D. W., Prokop, L. J., and Abu-Saleh, O. The proliferation of reports on clinical scoring systems: Issues about uptake and clinical utility. *JAMA*, 321(24):2405, June 2019. ISSN 0098-7444. doi: 10.1001/jama.2019.5284. URL <http://dx.doi.org/10.1001/jama.2019.5284>.

Champion, H. R., Sacco, W. J., Copes, W. S., Gann, D. S., Gennarelli, T. A., and Flanagan, M. E. A revision of the trauma score. *The Journal of Trauma: Injury, Infection, and Critical Care*, 29(5):623–629, May 1989. ISSN 0022-5282. doi: 10.1097/

00005373-198905000-00017. URL <http://dx.doi.org/10.1097/00005373-198905000-00017>.

Chen, I. Y., Pierson, E., Rose, S., Joshi, S., Ferryman, K., and Ghassemi, M. Ethical machine learning in healthcare. *Annual Review of Biomedical Data Science*, 4(1):123–144, July 2021. ISSN 2574-3414. doi: 10.1146/annurev-biodatasci-092820-114757. URL <http://dx.doi.org/10.1146/annurev-biodatasci-092820-114757>.

Chen, L. Overview of clinical prediction models. *Annals of Translational Medicine*, 8(4):71–71, February 2020. ISSN 2305-5847. doi: 10.21037/atm.2019.11.121. URL <http://dx.doi.org/10.21037/atm.2019.11.121>.

Chen, R. T. Q., Rubanova, Y., Bettencourt, J., and Duvenaud, D. K. Neural ordinary differential equations. In Bengio, S., Wallach, H., Larochelle, H., Grauman, K., Cesa-Bianchi, N., and Garnett, R. (eds.), *Advances in Neural Information Processing Systems*, volume 31. Curran Associates, Inc., 2018. URL https://proceedings.neurips.cc/paper_files/paper/2018/file/69386f6bb1dfed68692a24c8686939b9-Paper.pdf.

Collins, G. S., Reitsma, J. B., Altman, D. G., and Moons, K. G. Transparent reporting of a multivariable prediction model for individual prognosis or diagnosis (tripod): The tripod statement. *Annals of Internal Medicine*, 162(1): 55–63, January 2015. ISSN 1539-3704. doi: 10.7326/m14-0697. URL <http://dx.doi.org/10.7326/m14-0697>.

Cranmer, M. Interpretable machine learning for science with pysisr and symbolicregression.jl, 2023. URL <https://arxiv.org/abs/2305.01582>.

Dambha-Miller, H., Everitt, H., and Little, P. Clinical scores in primary care. *British Journal of General Practice*, 70 (693):163–163, March 2020. ISSN 1478-5242. doi: 10.3399/bjgp20X708941. URL <http://dx.doi.org/10.3399/bjgp20X708941>.

Dash, M. and Liu, H. Feature selection for classification. *Intelligent Data Analysis*, 1(1–4):131–156, 1997. ISSN 1088-467X. doi: 10.1016/s1088-467x(97)00008-5. URL [http://dx.doi.org/10.1016/s1088-467x\(97\)00008-5](http://dx.doi.org/10.1016/s1088-467x(97)00008-5).

Dawes, R. M. The robust beauty of improper linear models in decision making. *American Psychologist*, 34(7):571–582, July 1979. ISSN 0003-066X. doi: 10.1037/0003-066x.34.7.571. URL <http://dx.doi.org/10.1037/0003-066x.34.7.571>.

Desai, N. and Gross, J. Scoring systems in the critically ill: uses, cautions, and future directions. *BJA Education*, 19(7):212–218, 2019. ISSN 2058-5349. doi: 10.1016/j.bjae.2019.03.002. URL <http://dx.doi.org/10.1016/j.bjae.2019.03.002>.

Dimmer, A., Baird, R., and Puligandla, P. Role of practice standardization in outcome optimization for cdh. *World Journal of Pediatric Surgery*, 7(2):e000783, March 2024. ISSN 2516-5410. doi: 10.1136/wjps-2024-000783. URL <http://dx.doi.org/10.1136/wjps-2024-000783>.

Durack, D. T., Lukes, A. S., Bright, D. K., and Service, D. E. New criteria for diagnosis of infective endocarditis: utilization of specific echocardiographic findings. *The American Journal of Medicine*, 96(3):200–209, March 1994. ISSN 0002-9343. doi: 10.1016/0002-9343(94)90143-0. URL [http://dx.doi.org/10.1016/0002-9343\(94\)90143-0](http://dx.doi.org/10.1016/0002-9343(94)90143-0).

D'Agostino, R. B., Vasan, R. S., Pencina, M. J., Wolf, P. A., Cobain, M., Massaro, J. M., and Kannel, W. B. General cardiovascular risk profile for use in primary care: The framingham heart study. *Circulation*, 117(6): 743–753, February 2008. ISSN 1524-4539. doi: 10.1161/circulationaha.107.699579. URL <http://dx.doi.org/10.1161/CIRCULATIONAHA.107.699579>.

Esteva, A., Kuprel, B., Novoa, R. A., Ko, J., Swetter, S. M., Blau, H. M., and Thrun, S. Dermatologist-level classification of skin cancer with deep neural networks. *Nature*, 542(7639):115–118, January 2017. ISSN 1476-4687. doi: 10.1038/nature21056. URL <http://dx.doi.org/10.1038/nature21056>.

Gall, J.-R. L., Loirat, P., Alperovitch, A., Glaser, P., Granthil, C., Mathieu, D., Mercier, P., Thomas, R., and Villers, D. A simplified acute physiology score for icu patients. *Critical Care Medicine*, 12(11):975–977, November 1984. ISSN 0090-3493. doi: 10.1097/00003246-198411000-00012. URL <http://dx.doi.org/10.1097/00003246-198411000-00012>.

Gigerenzer, G. and Gaissmaier, W. Heuristic decision making. *Annual Review of Psychology*, 62 (1):451–482, January 2011. ISSN 1545-2085. doi: 10.1146/annurev-psych-120709-145346. URL <http://dx.doi.org/10.1146/annurev-psych-120709-145346>.

Goldstein, B. A., Navar, A. M., Pencina, M. J., and Ioannidis, J. P. A. Opportunities and challenges in developing risk prediction models with electronic health records data: a systematic review. *Journal of the American Medical Informatics Association*, 24(1):198–208, May 2016. ISSN

1527-974X. doi: 10.1093/jamia/ocw042. URL <http://dx.doi.org/10.1093/jamia/ocw042>.

Graham, R., Mancher, M., Miller Wolman, D., Greenfield, S., and Steinberg, E. *Clinical Practice Guidelines We Can Trust*. National Academies Press, Washington, DC, 2011. ISBN 9780309164232.

Granger, C. B. Predictors of hospital mortality in the global registry of acute coronary events. *Archives of Internal Medicine*, 163(19):2345, October 2003. ISSN 0003-9926. doi: 10.1001/archinte.163.19.2345. URL <http://dx.doi.org/10.1001/archinte.163.19.2345>.

Hager, P., Jungmann, F., Holland, R., Bhagat, K., Hubrecht, I., Knauer, M., Vielhauer, J., Makowski, M., Braren, R., Kaassis, G., and Rueckert, D. Evaluation and mitigation of the limitations of large language models in clinical decision-making. *Nature Medicine*, 30(9):2613–2622, July 2024. ISSN 1546-170X. doi: 10.1038/s41591-024-03097-1. URL <http://dx.doi.org/10.1038/s41591-024-03097-1>.

Hastie, T. and Tibshirani, R. Generalized additive models. *Statistical Science*, 1(3), August 1986. ISSN 0883-4237. doi: 10.1214/ss/1177013604. URL <http://dx.doi.org/10.1214/ss/1177013604>.

Hofer, I. S., Burns, M., Kendale, S., and Wanderer, J. P. Realistically integrating machine learning into clinical practice: A road map of opportunities, challenges, and a potential future. *Anesthesia & Analgesia*, 130(5):1115–1118, May 2020. ISSN 0003-2999. doi: 10.1213/ane.0000000000004575. URL <http://dx.doi.org/10.1213/ANE.0000000000004575>.

Hu, X., Rudin, C., and Seltzer, M. Optimal sparse decision trees. In Wallach, H., Larochelle, H., Beygelzimer, A., d'Alché-Buc, F., Fox, E., and Garnett, R. (eds.), *Advances in Neural Information Processing Systems*, volume 32. Curran Associates, Inc., 2019. URL https://proceedings.neurips.cc/paper_files/paper/2019/file/ac52c626afc10d4075708ac4c778ddfc-Paper.pdf.

Johnson, A. E. W., Bulgarelli, L., Shen, L., Gayles, A., Shammout, A., Horng, S., Pollard, T. J., Hao, S., Moody, B., Gow, B., Lehman, L.-w. H., Celi, L. A., and Mark, R. G. Mimic-iv, a freely accessible electronic health record dataset. *Scientific Data*, 10(1), January 2023. ISSN 2052-4463. doi: 10.1038/s41597-022-01899-x. URL <http://dx.doi.org/10.1038/s41597-022-01899-x>.

Kather, J. N., Heij, L. R., Grabsch, H. I., Loeffler, C., Echle, A., Muti, H. S., Krause, J., Niehues, J. M., Sommer, K. A. J., Bankhead, P., Kooreman, L. F. S., Schulte, J. J., Cipriani, N. A., Buelow, R. D., Boor, P., Ortiz-Brüchle, N., Hanby, A. M., Speirs, V., Kochanny, S., Patnaik, A., Srisuwananukorn, A., Brenner, H., Hoffmeister, M., van den Brandt, P. A., Jäger, D., Trautwein, C., Pearson, A. T., and Luedde, T. Pan-cancer image-based detection of clinically actionable genetic alterations. *Nature Cancer*, 1(8):789–799, July 2020. ISSN 2662-1347. doi: 10.1038/s43018-020-0087-6. URL <http://dx.doi.org/10.1038/s43018-020-0087-6>.

Kelly, C. J., Karthikesalingam, A., Suleyman, M., Corrado, G., and King, D. Key challenges for delivering clinical impact with artificial intelligence. *BMC Medicine*, 17(1), October 2019. ISSN 1741-7015. doi: 10.1186/s12916-019-1426-2. URL <http://dx.doi.org/10.1186/s12916-019-1426-2>.

Killock, D. Ai outperforms radiologists in mammographic screening. *Nature Reviews Clinical Oncology*, 17(3):134–134, January 2020. ISSN 1759-4782. doi: 10.1038/s41571-020-0329-7. URL <http://dx.doi.org/10.1038/s41571-020-0329-7>.

Kroenke, K., Spitzer, R. L., and Williams, J. B. W. The phq-9: Validity of a brief depression severity measure. *Journal of General Internal Medicine*, 16(9):606–613, September 2001. ISSN 1525-1497. doi: 10.1046/j.1525-1497.2001.016009606.x. URL <http://dx.doi.org/10.1046/j.1525-1497.2001.016009606.x>.

Kwong, J. C. C., Erdman, L., Khondker, A., Skreta, M., Goldenberg, A., McCradden, M. D., Lorenzo, A. J., and Rickard, M. The silent trial - the bridge between bench-to-bedside clinical ai applications. *Frontiers in Digital Health*, 4, August 2022. ISSN 2673-253X. doi: 10.3389/fdgth.2022.929508. URL <http://dx.doi.org/10.3389/fdgth.2022.929508>.

Letham, B., Rudin, C., McCormick, T. H., and Madigan, D. Interpretable classifiers using rules and bayesian analysis: Building a better stroke prediction model. *The Annals of Applied Statistics*, 9(3), September 2015. ISSN 1932-6157. doi: 10.1214/15-aos848. URL <http://dx.doi.org/10.1214/15-AOAS848>.

Lim, W S an van der Eerden, M. M., Laing, R., Boersma, W. G., Karalus, N., Town, G. I., Lewis, S. A., and Macfarlane, J. T. Defining community acquired pneumonia severity on presentation to hospital: an international derivation and validation study. *Thorax*, 58(5):377–382, May 2003. ISSN 0040-6376. doi: 10.1136/thorax.58.5.377. URL <http://dx.doi.org/10.1136/thorax.58.5.377>.

Lip, G. Y., Nieuwlaat, R., Pisters, R., Lane, D. A., and Crijns, H. J. Refining clinical risk stratification for pre-

dicting stroke and thromboembolism in atrial fibrillation using a novel risk factor-based approach. *Chest*, 137(2):263–272, February 2010. ISSN 0012-3692. doi: 10.1378/chest.09-1584. URL <http://dx.doi.org/10.1378/chest.09-1584>.

Lipton, Z. C. The mythos of model interpretability. *Communications of the ACM*, 61(10):36–43, September 2018. ISSN 1557-7317. doi: 10.1145/3233231. URL <http://dx.doi.org/10.1145/3233231>.

Liu, J., Zhong, C., Li, B., Seltzer, M., and Rudin, C. Faster-risk: Fast and accurate interpretable risk scores. In Oh, A. H., Agarwal, A., Belgrave, D., and Cho, K. (eds.), *Advances in Neural Information Processing Systems*, 2022. URL <https://openreview.net/forum?id=xTYL1J6Xt-z>.

Liu, T., Huynh, N., and van der Schaar, M. Decision tree induction through LLMs via semantically-aware evolution. In *The Thirteenth International Conference on Learning Representations*, 2025. URL <https://openreview.net/forum?id=UyhRtB4hjN>.

Lundberg, S. M. and Lee, S.-I. A unified approach to interpreting model predictions. In *Advances in Neural Information Processing Systems (NeurIPS)*, 2017.

Miller, G. A. The magical number seven, plus or minus two: Some limits on our capacity for processing information. *Psychological Review*, 63(2):81–97, March 1956. ISSN 0033-295X. doi: 10.1037/h0043158. URL <http://dx.doi.org/10.1037/h0043158>.

Molnar, C., König, G., Herbinger, J., Freiesleben, T., Dandl, S., Scholbeck, C. A., Casalicchio, G., Grosse-Wentrup, M., and Bischl, B. *General Pitfalls of Model-Agnostic Interpretation Methods for Machine Learning Models*, pp. 39–68. Springer International Publishing, 2022. ISBN 9783031040832. doi: 10.1007/978-3-031-04083-2_4. URL http://dx.doi.org/10.1007/978-3-031-04083-2_4.

Moons, K. G. M., Altman, D. G., Reitsma, J. B., and Collins, G. S. New guideline for the reporting of studies developing, validating, or updating a multi-variable clinical prediction model: The tripod statement. *Advances in Anatomic Pathology*, 22(5):303–305, September 2015. ISSN 1072-4109. doi: 10.1097/pap.0000000000000072. URL <http://dx.doi.org/10.1097/PAP.0000000000000072>.

Moons, K. G. M., Damen, J. A. A., Kaul, T., Hooft, L., Andaur Navarro, C., Dhirman, P., Beam, A. L., Van Calster, B., Celi, L. A., Denaxas, S., Denniston, A. K., Ghassemi, M., Heinze, G., Kengne, A. P., Maier-Hein, L., Liu, X., Logullo, P., McCradden, M. D., Liu, N., Oakden-Rayner, L., Singh, K., Ting, D. S., Wynants, L., Yang, B., Reitsma, J. B., Riley, R. D., Collins, G. S., and van Smeden, M. Probast+ai: an updated quality, risk of bias, and applicability assessment tool for prediction models using regression or artificial intelligence methods. *BMJ*, 388:e082505, March 2025. ISSN 1756-1833. doi: 10.1136/bmj-2024-082505. URL <http://dx.doi.org/10.1136/bmj-2024-082505>.

Nam, J., Kim, K., Oh, S., Tack, J., Kim, J., and Shin, J. Optimized feature generation for tabular data via LLMs with decision tree reasoning. In *The Thirty-eighth Annual Conference on Neural Information Processing Systems*, 2024. URL <https://openreview.net/forum?id=APSBwuMopO>.

Nori, H., Jenkins, S., Koch, P., and Caruana, R. InterpretML: A unified framework for machine learning interpretability, 2019. URL <https://arxiv.org/abs/1909.09223>.

Olesen, J., Torp-Pedersen, C., Hansen, M., and Lip, G. The value of the cha2ds2-vasc score for refining stroke risk stratification in patients with atrial fibrillation with a chads2 score 0–1: A nationwide cohort study. *Thrombosis and Haemostasis*, 107(06):1172–1179, 2012. ISSN 2567-689X. doi: 10.1160/th12-03-0175. URL <http://dx.doi.org/10.1160/TH12-03-0175>.

Pal, A., Umapathi, L. K., and Sankarasubbu, M. Medmcqa: A large-scale multi-subject multi-choice dataset for medical domain question answering. In Flores, G., Chen, G. H., Pollard, T., Ho, J. C., and Naumann, T. (eds.), *Proceedings of the Conference on Health, Inference, and Learning*, volume 174 of *Proceedings of Machine Learning Research*, pp. 248–260. PMLR, 07–08 Apr 2022. URL <https://proceedings.mlr.press/v174/pal22a.html>.

Patton, D. D. Introduction to clinical decision making. *Seminars in Nuclear Medicine*, 8(4):273–282, October 1978. ISSN 0001-2998. doi: 10.1016/s0001-2998(78)80013-0. URL [http://dx.doi.org/10.1016/s0001-2998\(78\)80013-0](http://dx.doi.org/10.1016/s0001-2998(78)80013-0).

Pollard, T. J., Johnson, A. E. W., Raffa, J. D., Celi, L. A., Mark, R. G., and Badawi, O. The eicu collaborative research database, a freely available multi-center database for critical care research. *Scientific Data*, 5(1), September 2018. ISSN 2052-4463. doi: 10.1038/sdata.2018.178. URL <http://dx.doi.org/10.1038/sdata.2018.178>.

Ramos, K. J., Quon, B. S., Heltshe, S. L., Mayer-Hamblett, N., Lease, E. D., Aitken, M. L., Weiss, N. S., and Goss, C. H. Heterogeneity in survival in adult patients with cystic fibrosis with fev1 under 30 *Chest*,

151(6):1320–1328, June 2017. ISSN 0012-3692. doi: 10.1016/j.chest.2017.01.019. URL <http://dx.doi.org/10.1016/j.chest.2017.01.019>.

Ramos, K. J., Smith, P. J., McKone, E. F., Pilewski, J. M., Lucy, A., Hempstead, S. E., Tallarico, E., Faro, A., Rosenbluth, D. B., Gray, A. L., and Dunitz, J. M. Lung transplant referral for individuals with cystic fibrosis: Cystic fibrosis foundation consensus guidelines. *Journal of Cystic Fibrosis*, 18(3):321–333, May 2019. ISSN 1569-1993. doi: 10.1016/j.jcf.2019.03.002. URL <http://dx.doi.org/10.1016/j.jcf.2019.03.002>.

Ribeiro, M. T., Singh, S., and Guestrin, C. "why should i trust you?": Explaining the predictions of any classifier. In *Proceedings of the 22nd ACM SIGKDD International Conference on Knowledge Discovery and Data Mining*, KDD '16, pp. 1135–1144, New York, NY, USA, 2016. Association for Computing Machinery. ISBN 9781450342322. doi: 10.1145/2939672.2939778. URL <https://doi.org/10.1145/2939672.2939778>.

Royal College of Physicians. National early warning score (news) 2. Official guideline report, 2017. URL <https://www.rcp.ac.uk/improving-care/resources/national-early-warning-score-news-2/>.

Rudin, C. Stop explaining black box machine learning models for high stakes decisions and use interpretable models instead. *Nature Machine Intelligence*, 1(5):206–215, May 2019. ISSN 2522-5839. doi: 10.1038/s42256-019-0048-x. URL <http://dx.doi.org/10.1038/s42256-019-0048-x>.

Shell, I. G. Decision rules for the use of radiography in acute ankle injuries: Refinement and prospective validation. *JAMA*, 269(9):1127, March 1993. ISSN 0098-7484. doi: 10.1001/jama.1993.03500090063034. URL <http://dx.doi.org/10.1001/jama.1993.03500090063034>.

Shickel, B., Tighe, P. J., Bihorac, A., and Rashidi, P. Deep ehr: A survey of recent advances in deep learning techniques for electronic health record (ehr) analysis. *IEEE Journal of Biomedical and Health Informatics*, 22(5):1589–1604, September 2018. ISSN 2168-2208. doi: 10.1109/jbhi.2017.2767063. URL <http://dx.doi.org/10.1109/JBHI.2017.2767063>.

Shortliffe, E. H. and Sepulveda, M. J. Clinical decision support in the era of artificial intelligence. *JAMA*, 320(21):2199, December 2018. ISSN 0098-7484. doi: 10.1001/jama.2018.17163. URL <http://dx.doi.org/10.1001/jama.2018.17163>.

Silva, I., Moody, G., Scott, D. J., Celi, L. A., and Mark, R. G. Predicting in-hospital mortality of icu patients: The physionet/computing in cardiology challenge 2012. *Computing in cardiology*, 39:245–248, 2012. ISSN 2325-8861. URL <https://europepmc.org/articles/PMC3965265>.

Silverman, W. A. and Andersen, D. H. A controlled clinical trial of effects of water mist on obstructive respiratory signs, death rate and necropsy findings among premature infants. *Pediatrics*, 17(1):1–10, 1956.

Singer, M., Deutschman, C. S., Seymour, C. W., Shankar-Hari, M., Annane, D., Bauer, M., Bellomo, R., Bernard, G. R., Chiche, J.-D., Coopersmith, C. M., Hotchkiss, R. S., Levy, M. M., Marshall, J. C., Martin, G. S., Opal, S. M., Rubenfeld, G. D., van der Poll, T., Vincent, J.-L., and Angus, D. C. The third international consensus definitions for sepsis and septic shock (sepsis-3). *JAMA*, 315(8):801, February 2016. ISSN 0098-7484. doi: 10.1001/jama.2016.0287. URL <http://dx.doi.org/10.1001/jama.2016.0287>.

Singhal, K., Azizi, S., Tu, T., Mahdavi, S. S., Wei, J., Chung, H. W., Scales, N., Tanwani, A., Cole-Lewis, H., Pfohl, S., Payne, P., Seneviratne, M., Gamble, P., Kelly, C., Babiker, A., Schärli, N., Chowdhery, A., Mansfield, P., Demner-Fushman, D., Agüera y Arcas, B., Webster, D., Corrado, G. S., Matias, Y., Chou, K., Gottweis, J., Tomasev, N., Liu, Y., Rajkomar, A., Barral, J., Semturs, C., Karthikesalingam, A., and Natarajan, V. Large language models encode clinical knowledge. *Nature*, 620(7972):172–180, July 2023. ISSN 1476-4687. doi: 10.1038/s41586-023-06291-2. URL <http://dx.doi.org/10.1038/s41586-023-06291-2>.

Steyerberg, E. W., Vickers, A. J., Cook, N. R., Gerds, T., Gonen, M., Obuchowski, N., Pencina, M. J., and Kattan, M. W. Assessing the performance of prediction models: A framework for traditional and novel measures. *Epidemiology*, 21(1):128–138, January 2010. ISSN 1044-3983. doi: 10.1097/ede.0b013e3181c30fb2. URL <http://dx.doi.org/10.1097/EDe.0b013e3181c30fb2>.

Sullivan, L. M., Massaro, J. M., and D'Agostino, R. B. Presentation of multivariate data for clinical use: The framingham study risk score functions. *Statistics in Medicine*, 23(10):1631–1660, April 2004. ISSN 1097-0258. doi: 10.1002/sim.1742. URL <http://dx.doi.org/10.1002/sim.1742>.

Sur, R. and Dahm, P. History of evidence-based medicine. *Indian Journal of Urology*, 27(4):487, 2011. ISSN 0970-1591. doi: 10.4103/0970-1591.91438. URL <http://dx.doi.org/10.4103/0970-1591.91438>.

Takita, H., Kabata, D., Walston, S. L., Tatekawa, H., Saito, K., Tsujimoto, Y., Miki, Y., and Ueda, D. A systematic review and meta-analysis of diagnostic performance comparison between generative ai and physicians. *npj Digital Medicine*, 8(1), March 2025. ISSN 2398-6352. doi: 10.1038/s41746-025-01543-z. URL <http://dx.doi.org/10.1038/s41746-025-01543-z>.

Teasdale, G. and Jennett, B. Assessment of coma and impaired consciousness. *The Lancet*, 304(7872):81–84, July 1974. ISSN 0140-6736. doi: 10.1016/s0140-6736(74)91639-0. URL [http://dx.doi.org/10.1016/s0140-6736\(74\)91639-0](http://dx.doi.org/10.1016/s0140-6736(74)91639-0).

Topol, E. J. High-performance medicine: the convergence of human and artificial intelligence. *Nature Medicine*, 25(1):44–56, January 2019. ISSN 1546-170X. doi: 10.1038/s41591-018-0300-7. URL <http://dx.doi.org/10.1038/s41591-018-0300-7>.

Ustun, B. and Rudin, C. Supersparse linear integer models for optimized medical scoring systems. *Machine Learning*, 102(3):349–391, November 2015. ISSN 1573-0565. doi: 10.1007/s10994-015-5528-6. URL <http://dx.doi.org/10.1007/s10994-015-5528-6>.

Ustun, B. and Rudin, C. Learning optimized risk scores. *Journal of Machine Learning Research*, 20(150):1–75, 2019. URL <http://jmlr.org/papers/v20/18-615.html>.

Vincent, J.-L. and Moreno, R. Clinical review: Scoring systems in the critically ill. *Critical Care*, 14(2):207, 2010. ISSN 1364-8535. doi: 10.1186/cc8204. URL <http://dx.doi.org/10.1186/cc8204>.

Vincent, J. L., Moreno, R., Takala, J., Willatts, S., De Mendonça, A., Bruining, H., Reinhart, C. K., Suter, P. M., and Thijs, L. G. The sofa (sepsis-related organ failure assessment) score to describe organ dysfunction/failure: On behalf of the working group on sepsis-related problems of the european society of intensive care medicine (see contributors to the project in the appendix). *Intensive Care Medicine*, 22(7):707–710, July 1996. ISSN 1432-1238. doi: 10.1007/bf01709751. URL <http://dx.doi.org/10.1007/BF01709751>.

Wang, F. The crisis of biomedical foundation models. *Journal of Biomedical Informatics*, 171:104917, November 2025. ISSN 1532-0464. doi: 10.1016/j.jbi.2025.104917. URL <http://dx.doi.org/10.1016/j.jbi.2025.104917>.

Wasylewicz, A. T. M. and Scheepers-Hoeks, A. M. J. W. *Clinical Decision Support Systems*. Springer International Publishing, December 2018. ISBN 9783319997131. doi: 10.1007/978-3-319-99713-1_11. URL http://dx.doi.org/10.1007/978-3-319-99713-1_11.

Welch, J., Dean, J., and Hartin, J. Using news2: an essential component of reliable clinical assessment. *Clinical Medicine*, 22(6):509–513, November 2022. ISSN 1470-2118. doi: 10.7861/clinmed.2022-0435. URL <http://dx.doi.org/10.7861/clinmed.2022-0435>.

Wells, P., Anderson, D., Rodger, M., Ginsberg, J., Kearon, C., Gent, M., Turpie, A., Bormanis, J., Weitz, J., Chamberlain, M., Bowie, D., Barnes, D., and Hirsh, J. Derivation of a simple clinical model to categorize patients probability of pulmonary embolism: Increasing the models utility with the simplified d-dimer. *Thrombosis and Haemostasis*, 83(03):416–420, 2000. ISSN 2567-689X. doi: 10.1055/s-0037-1613830. URL <http://dx.doi.org/10.1055/s-0037-1613830>.

Wells, P. S., Anderson, D. R., Bormanis, J., Guy, F., Mitchell, M., Gray, L., Clement, C., Robinson, K. S., and Lewandowski, B. Value of assessment of pretest probability of deep-vein thrombosis in clinical management. *The Lancet*, 350(9094):1795–1798, December 1997. ISSN 0140-6736. doi: 10.1016/s0140-6736(97)08140-3. URL [http://dx.doi.org/10.1016/s0140-6736\(97\)08140-3](http://dx.doi.org/10.1016/s0140-6736(97)08140-3).

Wieten, S. Expertise in evidence-based medicine: a tale of three models. *Philosophy, Ethics, and Humanities in Medicine*, 13(1), February 2018. ISSN 1747-5341. doi: 10.1186/s13010-018-0055-2. URL <http://dx.doi.org/10.1186/s13010-018-0055-2>.

Williams, C. Y. K., Miao, B. Y., Kornblith, A. E., and Butte, A. J. Evaluating the use of large language models to provide clinical recommendations in the emergency department. *Nature Communications*, 15(1), October 2024. ISSN 2041-1723. doi: 10.1038/s41467-024-52415-1. URL <http://dx.doi.org/10.1038/s41467-024-52415-1>.

Wolff, R. F., Moons, K. G., Riley, R. D., Whiting, P. F., Westwood, M., Collins, G. S., Reitsma, J. B., Kleijnen, J., and Mallett, S. Probst: A tool to assess the risk of bias and applicability of prediction model studies. *Annals of Internal Medicine*, 170(1):51–58, January 2019. ISSN 1539-3704. doi: 10.7326/m18-1376. URL <http://dx.doi.org/10.7326/m18-1376>.

Woolf, S. H., Grol, R., Hutchinson, A., Eccles, M., and Grimshaw, J. Clinical guidelines: Potential benefits, limitations, and harms of clinical guidelines. *BMJ*, 318(7182):527–530, February 1999. ISSN 1468-5833. doi: 10.1136/bmj.318.7182.527. URL <http://dx.doi.org/10.1136/bmj.318.7182.527>.

Xie, F., Chakraborty, B., Ong, M. E. H., Goldstein, B. A., and Liu, N. Autoscore: A machine learning-based automatic clinical score generator and its application

to mortality prediction using electronic health records.
JMIR Medical Informatics, 8(10):e21798, October 2020.
ISSN 2291-9694. doi: 10.2196/21798. URL <http://dx.doi.org/10.2196/21798>.

Zhong, D., Wu, Y., Aarons, G. A., Hutchinson, A. M., Wong, W. C., Lv, S., Song, Z., Wu, Y., Bishai, D. M., Chen, K., Yang, N., Chen, Y., Liu, Z., Yan, L., Zhou, P., and Xu, D. R. Implementability of clinical practice guidelines: the review and development of a comprehensive framework for guideline implementability (cfgi). *Implementation Science Communications*, 6 (1), October 2025. ISSN 2662-2211. doi: 10.1186/s43058-025-00780-3. URL <http://dx.doi.org/10.1186/s43058-025-00780-3>.

Supplementary Material for AgentScore

A. Clinical scoring systems

A.1. Why clinical scoring systems matter

Role in evidence-based medicine and workflow standardization. In routine clinical practice, guidelines function as operational coordination mechanisms that determine how evidence is applied across heterogeneous clinicians, settings, and time horizons, often under conditions of uncertainty and time pressure (Welch et al., 2022; Dimmer et al., 2024). Their effectiveness depends not only on statistical validity, but on whether recommendations can be executed reliably at the bedside using routinely available information, frequently by clinicians with differing levels of training (Graham et al., 2011). As a result, guideline impact in real-world workflows is driven less by marginal improvements in predictive accuracy than by the ability to produce decisions that are consistent, auditable, and directly actionable (Zhong et al., 2025).

Clinical scoring systems instantiate these principles by mapping a small number of routinely collected patient features to discrete risk strata or management recommendations. By coupling bounded integer scores to explicit action thresholds (e.g., hospital admission, advanced imaging, antibiotic administration), they provide a shared decision representation that supports triage, escalation, and communication across care settings (Dambha-Miller et al., 2020; Olesen et al., 2012; Vincent & Moreno, 2010). Crucially, these scores are embedded directly into care pathways rather than interpreted as unconstrained predictive outputs.

Why small, explicit rules survive deployment. From a learning-theoretic perspective, clinical deployment induces a mismatch between hypothesis classes that are easy to optimize and those that are viable in practice (Wang, 2025). High-capacity models benefit from smooth parameterizations and weak structural constraints, enabling efficient optimization and strong retrospective performance. In contrast, bedside deployment restricts models to discrete, low-capacity, and tightly structured forms that must be executed reliably under time pressure and partial information (Graham et al., 2011).

Under these constraints, additional model flexibility often yields diminishing returns with respect to clinically actionable decision quality (Chen, 2020; Steyerberg et al., 2010). Instead, compact rule-based models operate near the boundary of minimal sufficient complexity: by excluding degrees of freedom that cannot be supported at deployment time, they exhibit improved robustness to sampling variability, distribution shift, and execution noise (Dash & Liu, 1997; Wasylewicz & Scheepers-Hoeks, 2018). Their enduring use in clinical practice reflects an implicit optimization objective—maximize performance subject to hard constraints on executability and stability, rather than unconstrained predictive accuracy.

A.2. Case studies of clinical impact

Clinical scoring systems achieve impact not merely by ranking risk, but by reliably changing clinical decisions through explicit, thresholded actions. Table 5 summarizes the checklist structure of four widely adopted decision rules that illustrate complementary mechanisms of clinical impact. Across all cases, clinical impact arises from the presence of trusted, explicit action thresholds that deterministically link observed findings to management decisions. Their enduring adoption reflects the value of compact, unit-weighted checklists in converting uncertainty into reliable action, rather than marginal improvements in discriminative accuracy alone.

Acute care escalation tools such as qSOFA (Singer et al., 2016) and CURB-65 (Lim et al., 2003) provide rapid bedside identification of patients at elevated risk of deterioration or mortality. By mapping a small number of routinely available observations to discrete severity thresholds, these scores support timely escalation, admission decisions, and resource allocation under conditions of uncertainty. In primary care, the Centor criteria illustrate a complementary mechanism: by aggregating a small set of binary clinical findings into a bounded checklist, the score supports rational antibiotic prescribing and targeted diagnostic testing, reducing unnecessary treatment while maintaining safety. The Ottawa Ankle Rules (Shell, 1993) demonstrate a distinct but equally important form of impact in emergency medicine, where a conservative binary checklist enables the safe exclusion of fracture and avoids unnecessary imaging, reducing cost and patient burden without increasing missed injuries. For the Ottawa Ankle Rules, the checklist is operationalized as a conservative OR-rule.

Table 5. Binary checklist structure of representative clinical decision rules. Each system consists of unit-weighted binary conditions (+1 if satisfied) whose total score is mapped to an explicit guideline-recommended clinical action.

Score	Item	Binary rule (satisfied?)	Points
qSOFA	Respiratory rate	Respiratory rate \geq 22 breaths/min	+1
	Blood pressure	Systolic blood pressure \leq 100 mmHg	+1
	Mental status	Altered mental status (GCS < 15)	+1
	<i>Threshold & action</i>	Score $\geq 2 \Rightarrow$ high risk of sepsis; urgent evaluation	
CURB-65	Confusion	New onset confusion (disorientation to person, place, or time)	+1
	Urea	Blood urea nitrogen $> 7 \text{ mmol/L}$	+1
	Respiratory rate	Respiratory rate $\geq 30 \text{ breaths/min}$	+1
	Blood pressure	Systolic $< 90 \text{ mmHg}$ or diastolic $\leq 60 \text{ mmHg}$	+1
	Age	Age $\geq 65 \text{ years}$	+1
	<i>Threshold & action</i>	Score $\geq 3 \Rightarrow$ inpatient management recommended	
Centor	Fever	History of fever or measured temperature $\geq 38^\circ\text{C}$	+1
	Tonsillar exudates	Tonsillar exudates or swelling present	+1
	Cervical lymphadenopathy	Tender anterior cervical lymph nodes	+1
	Cough absence	Absence of cough	+1
	<i>Threshold & action</i>	Score $\geq 3 \Rightarrow$ consider antibiotics or rapid strep testing	
Ottawa Ankle Rules	Malleolar pain	Pain in the malleolar zone	+1
	Bone tenderness (lateral)	Tenderness at posterior edge or tip of lateral malleolus	+1
	Bone tenderness (medial)	Tenderness at posterior edge or tip of medial malleolus	+1
	Weight bearing (immediate)	Inability to bear weight immediately after injury	+1
	Weight bearing (ED)	Inability to bear weight for four steps in the hospital	+1
	<i>Threshold & action</i>	Score $\geq 1 \Rightarrow$ ankle radiography indicated	

A.3. Survey of established guideline scores

Scope. To contextualize our modeling choices, we examined a range of widely adopted clinical scoring systems spanning acute care, cardiology, respiratory disease, obstetrics, psychiatry, and trauma (Table 6). We focused on scores that are guideline-embedded, widely cited, and routinely used in clinical practice. Despite their diverse clinical contexts and historical origins, these systems exhibit a remarkably consistent design philosophy, suggesting the presence of shared, domain-agnostic deployment constraints.

Common structural properties. Across domains, successful clinical scoring systems share several recurring features: (i) a small number of easily recalled items (typically 5–10); (ii) reliance on routine, low-cost inputs; (iii) integer or low-cardinality scoring that enables manual computation; (iv) bounded score ranges that support clear risk stratification; and (v) explicit thresholds tied to concrete management actions. Together, these properties promote robustness to missingness, reduce cognitive burden, and enable reliable execution without specialized infrastructure.

Implications for hypothesis class design. These empirical regularities motivate learning directly within the checklist structures observed in deployed guidelines, rather than approximating them post hoc. In particular, across surveyed systems the median checklist length is five, with the majority of widely deployed scores operating at six or fewer items (Table 6). This concentration at small rule counts supports treating a limited rule budget as a deployability prior rather than a tunable performance parameter. Restricting the rule budget regularizes the hypothesis class, limits cognitive load, and aligns model structure with real-world guideline practice. This is also consistent with classic results on the limits of human working memory, suggesting that compact checklists better match the cognitive constraints of bedside decision-making (Miller, 1956).

Similarly, restricting attention to unit-weighted rules is supported by both clinical convention and classical results on improper linear models, which show that equal-weighted predictors often perform competitively in noisy, low-signal regimes while exhibiting greater robustness to estimation error (Dawes, 1979). While some successful scores employ non-unit weights, their increased arithmetic complexity frequently necessitates reference aids. When a unit-weighted formulation is feasible, it is therefore preferable due to reduced arithmetic burden and more reliable bedside execution.

Taken together, these considerations justify focusing on compact, unit-weighted checklists as the most expressive hypothesis class that remains reliably deployable under realistic clinical conditions.

Table 6. Overview of established clinical scoring systems. Widely adopted scores rely on a small number of routine features, integer or categorical point allocations, and explicit decision thresholds, enabling memorability and bedside deployment without specialized infrastructure.

Domain	Score	# Items	Range	Typical use / threshold	Reference
Infection / Sepsis	SIRS	4	0–4	≥ 2: systemic inflammation	(Bone et al., 1992)
Thrombosis	Wells (DVT)	9	0–9	≥ 2: high DVT probability	(Wells et al., 1997)
	Wells (PE)	7	0–12.5	≥ 4: high PE probability	(Wells et al., 2000)
Cardiology	CHA ₂ DS ₂ -VASc	8	0–9	≥ 2: anticoagulation	(Lip et al., 2010)
	GRACE	8	0–15	ACS mortality risk	(Granger, 2003)
	Framingham	9	0–30	10-year cardiovascular risk	(D'Agostino et al., 2008)
Respiratory	CURB-65	5	0–5	≥ 3: inpatient management	(Lim et al., 2003)
	Centor	4	0–4	≥ 3: consider antibiotics	(Centor et al., 1981)
Gastrointestinal	Glasgow–Blatchford	8	0–23	≥ 1: urgent endoscopy	(Blatchford et al., 2000)
Neurology	Glasgow Coma Scale	3	3–15	≤ 8: severe head injury	(Teasdale & Jennett, 1974)
Psychiatry	PHQ-9	9	0–27	≥ 10: moderate depression	(Kroenke et al., 2001)
Obstetrics / Neonatal	Bishop Score	5	0–13	≥ 8: induction readiness	(Bishop, 1964)
	Silverman–Andersen	5	0–10	≥ 7: respiratory distress	(Silverman & Andersen, 1956)
Critical Care	SOFA	6	0–24	≥ 2: organ dysfunction	(Vincent et al., 1996)
	NEWS2	6	0–20	≥ 5: urgent clinical review	(Royal College of Physicians, 2017)
	qSOFA	3	0–3	≥ 2: sepsis risk trigger	(Singer et al., 2016)
Trauma / Imaging	RTS	4	0–8	≥ 2: trauma team activation	(Champion et al., 1989)
	Ottawa Ankle Rules	5	0–5	≥ 1: ankle radiography	(Shell, 1993)

B. The Clinical Scoring System Rule Grammar

Our rule language is designed to capture the *forms of reasoning that already survive deployment* in clinical guidelines: rules must be actionable (paired with clear thresholds), auditable (each condition can be inspected and contested), compute-free at the bedside (no continuous inference pipeline), and compatible with routine documentation and measurement practices (Woolf et al., 1999; Graham et al., 2011; Shortliffe & Sepulveda, 2018; Rudin, 2019; Moons et al., 2015). Accordingly, we restrict attention to a small set of rule families that recur across widely adopted scoring systems.

(i) Numeric thresholds: cutpoints as operational triggers. Clinical guidelines frequently operationalize physiologic risk through thresholded cutpoints that map directly to escalation actions. For example, CURB-65 uses a urea cutpoint (blood urea nitrogen > 7 mmol/L) and a respiratory rate cutpoint (≥ 30 breaths/min) to define higher-severity pneumonia and guide inpatient management (Lim et al., 2003). Similarly, qSOFA uses binary thresholds (e.g., respiratory rate ≥ 22 /min; systolic blood pressure ≤ 100 mmHg) as a sepsis risk trigger (Singer et al., 2016). In practice, such thresholds are robust to moderate measurement noise and are easy to execute at the bedside, motivating the inclusion of single-variable threshold rules as a primitive in \mathcal{R} .

(ii) Numeric ranges: normality bands and safety windows. Many physiologic variables exhibit *both* low- and high-risk regimes, and guidelines often reason in terms of safe bands or abnormality windows rather than monotone risk. Early warning scores, including NEWS2, discretize vital signs into clinically meaningful ranges (e.g., oxygen saturation bands, temperature bands, and systolic blood pressure bands) that reflect nonlinear risk and guide escalation (Royal College of Physicians, 2017). Range rules therefore provide a compact mechanism to encode “normal vs abnormal” intervals without introducing nontransparent nonlinearities.

(iii) Categorical inclusion and (iv) binary presence: yes/no clinical facts. Guideline logic often depends on discrete clinical facts—diagnoses, comorbidities, and prior events—that are naturally represented as categorical inclusion or binary presence rules. For instance, CHA₂DS₂-VASc assigns points for discrete risk factors such as diabetes mellitus, prior

stroke/TIA/thromboembolism, vascular disease, and heart failure (Lip et al., 2010; Olesen et al., 2012). Similarly, the Wells criteria include categorical items such as active cancer and recent immobilization/surgery (Wells et al., 1997). These variables are typically well documented in routine care and map cleanly to checklist items, motivating explicit support for categorical and binary predicates.

(v) Ratios and contrasts: derived physiology with long precedent. Clinicians frequently reason in *derived indices* that normalize or compare measurements rather than relying on raw values alone. Although many guideline scores encode derived reasoning implicitly via multiple thresholded items, the underlying clinical logic often corresponds to ratios or contrasts (e.g., oxygenation indices such as $\text{PaO}_2/\text{FiO}_2$, perfusion indices, or relative changes between related labs). Our language therefore permits a restricted allowlist of simple transformations (ratios and differences) to capture such reasoning while preserving interpretability and auditability. Importantly, these derived quantities are typically available at no additional cognitive or computational cost, as they can be precomputed automatically when the relevant laboratory measurements are ordered and results returned. We do not allow arbitrary algebraic expressions: only clinically interpretable forms (e.g., x_a/x_b or $x_a - x_b$) are permitted, and all derived rules are validated empirically and screened for plausibility by the eliminative plausibility agent.

(vi) Count-based rules: syndromic criteria and cumulative burden. Many clinical definitions and escalation triggers are inherently *M-of-N* criteria: the presence of multiple abnormal findings jointly increases suspicion or defines a syndrome. Classic examples include SIRS-style criteria, which combine several abnormal vitals/labs, and organ dysfunction frameworks such as SOFA, which aggregate multiple organ-specific components (Bone et al., 1992; Vincent et al., 1996). A widely taught diagnostic example is the Duke criteria for infective endocarditis, which require combinations of major and minor criteria to establish or exclude diagnosis, illustrating how guideline reasoning often formalizes evidence accumulation as transparent count-based logic (Durack et al., 1994). Count-based rules preserve transparency because the contributing items remain explicit and auditable; they also align naturally with unit-weighted checklist execution by capturing cumulative burden without complex arithmetic.

(vii) Shallow logical composition: small conjunctions/disjunctions mirror guideline logic. Guidelines often specify short conjunctions and disjunctions that define an abnormality or escalation trigger. For example, CURB-65 assigns a point for hypotension defined as *systolic* blood pressure < 90 **or** *diastolic* ≤ 60 mmHg (Lim et al., 2003), and the Wells criteria include a competing-diagnosis clause (“alternative diagnosis at least as likely”) that explicitly modifies the risk assessment (Wells et al., 1997). We therefore allow shallow AND/OR compositions over base predicates while restricting logical depth to preserve memorability and reduce execution error under time pressure (Miller, 1956; Gigerenzer & Gaissmaier, 2011).

(viii) Temporal and distributional summaries: capturing acuity and trend without black-box time-series. Clinical deterioration is often defined by *trends* rather than static values (e.g., rapid worsening, sustained abnormalities, or recent changes). In practice, many guideline tools operationalize time indirectly through repeated observations and escalation thresholds (e.g., repeated NEWS2 scoring over time) (Royal College of Physicians, 2017). To capture such reasoning while remaining compute-free at deployment, we restrict temporal constructs to simple, auditable summaries over a pre-index window (e.g., delta, percent change, range, or max–min). Canonical examples include acute kidney injury (AKI), where diagnostic criteria depend on changes in serum creatinine over time (e.g., a rise from baseline within a short window) rather than a single absolute measurement (Bellomo et al., 2004). Similar trend-based reasoning appears in myocardial infarction evaluation, where serial troponin measurements are interpreted through rises and/or falls over time, and in sepsis management, where lactate clearance (a decrease in lactate over a specified interval) is used to assess response to resuscitation and ongoing risk. More broadly, clinicians routinely monitor temporal patterns such as the fever curve (persistence or trajectory of temperature) when assessing infection progression or treatment response. All temporal features are computed using only measurements available prior to the prediction time to avoid label leakage.

Clinically meaningful discretization. To avoid spurious cutpoints and improve interpretability, continuous thresholds are quantized to clinically meaningful values (e.g., integer vitals, common lab units, or guideline-style bands), consistent with classical regression-to-points approaches used in clinical score construction (Sullivan et al., 2004). This discretization stabilizes rules under sampling variability and supports reliable bedside execution.

Missingness and measurement frequency. EHR data are characterized by irregular sampling and informative missingness. To ensure deployability and avoid hidden imputation effects, we define explicit missingness semantics for each rule family and report them alongside learned checklists. Concretely, if a required input is missing at prediction time, the rule evaluates to false by default, avoiding hidden imputation and preserving conservative, audit-friendly behavior under missingness.

C. Extended Related Work

C.1. Clinical scoring systems and score construction

Expert-designed scoring systems. A large fraction of widely used clinical scores are developed through expert consensus and guideline processes rather than direct optimization on large datasets. Such scores typically encode domain knowledge and pragmatic workflow constraints (e.g., reliance on routinely available measurements, bounded item counts, and actionable thresholds) and thus benefit from strong face validity, institutional trust, and straightforward bedside execution. In evidence-based medicine, these properties are not incidental: guidelines function as coordination mechanisms that standardize decisions across heterogeneous clinicians and settings, and therefore prioritize auditability and actionability alongside predictive utility (Woolf et al., 1999). The limitations are equally well known: expert-derived scores can be conservative, slow to update as evidence evolves, and may underperform in new populations or under distribution shift, especially when derived from small cohorts or historical practice patterns (Challener et al., 2019). These concerns are now formalized in clinical prediction model methodology through reporting and bias-assessment frameworks such as TRIPOD and PROBAST which emphasize transparency, applicability, and robustness under dataset shift (Collins et al., 2015; Wolff et al., 2019).

Regression-based score derivation and rounding. A classical approach to score construction fits a regression model (often logistic regression) and converts continuous coefficients into an integer point system via scaling and rounding, as exemplified by Framingham-style risk scores (Sullivan et al., 2004). This pipeline preserves the additive structure of linear predictors while producing a human-usable point tally, and it is often accompanied by calibration to produce risk estimates. However, coefficient-to-point conversion introduces additional approximation error, and the resulting point weights are typically non-unit and heterogeneous, imposing arithmetic burden and reducing memorability. Moreover, estimated coefficients may be unstable under sampling variability, collinearity, and missingness mechanisms, leading to sensitivity in the derived point system and thresholds across cohorts (Sullivan et al., 2004; Moons et al., 2015). These issues are particularly salient when scores are intended for manual computation or when guideline governance requires stable, transparent rules that remain sensible across institutions.

Optimization-based integer scoring methods. Recent work has formalized score construction as an optimization problem over sparse integer-weighted linear models, enabling direct control over sparsity, coefficient bounds, and (in some cases) monotonicity or sign constraints. Representative examples include AutoScore, which combines feature ranking and discretization with scorecard-style point assignment; RiskSLIM, which solves a mixed-integer program to optimize a sparse integer score; and FasterRisk, which provides a scalable approximation procedure for learning sparse risk scores under coefficient and sparsity constraints (Xie et al., 2020; Ustun & Rudin, 2015; Liu et al., 2022). These methods offer substantial advantages over ad hoc rounding: they search over discrete coefficient spaces directly and provide clearer objective-driven trade-offs. Nonetheless, they remain fundamentally *selectors* over a pre-specified feature matrix; in practice, this requires committing to a fixed set of binned threshold indicators and does not address the *generation-selection* gap when the clinically meaningful hypothesis class includes derived quantities, temporal summaries, or shallow compositional logic that are not explicitly available as features. Further, even when coefficients are small integers, heterogeneous weights typically require nontrivial arithmetic at the bedside and do not inherently yield checklist-style *N-of-M* decision procedures.

Why integer coefficients alone are insufficient. While integer coefficients increase interpretability relative to continuous weights, *integer* does not imply *deployable-by-design*. These human-factors limitations are increasingly recognized in clinical AI evaluation guidelines, which stress that executable decision procedures must be assessed in context of use rather than solely via retrospective accuracy metrics (Moons et al., 2025; Kwong et al., 2022). Heterogeneous point values still impose cognitive load and increase the risk of arithmetic errors under interruption and time pressure, and they often require external aids (charts, calculators, or EHR integration) for reliable execution. *There are, however, settings where heterogeneous integer weights are entirely appropriate:* for example, in longitudinal risk stratification and care planning where decisions are made with more time, or when scores are routinely pre-computed by software (e.g., EHR dashboards or clinical decision support systems), so the human does not perform arithmetic at the point of care. In these contexts, the added flexibility of non-unit integer weights can improve calibration or risk separation without materially increasing workflow burden. The central issue is therefore not whether weights are integer, but whether the computation and decision procedure are *bedside-executable* under realistic operating conditions.

In contrast, unit-weighted checklists align with how clinicians frequently reason in practice: as short sets of explicit triggers where the contribution of each rule is identical and the decision reduces to a count exceeding a threshold. This design is

also supported by classical results on so-called improper linear models, which show that equal-weighted predictors can be competitive in noisy regimes and may be more robust to estimation error than finely tuned weights (Dawes, 1979). From a human-factors standpoint, bounded item counts and simple aggregation rules (including N -of- M procedures) help accommodate working-memory constraints and facilitate consistent application in high-stakes environments (Miller, 1956; Gigerenzer & Gaissmaier, 2011). Finally, integer-score learners typically inherit the expressivity limits of their pre-binning: if clinically meaningful constructs are absent from the initial feature representation, coefficient optimization alone cannot recover them.

C.2. Interpretable machine learning

Inherently interpretable models. Inherently interpretable models aim to make the full predictive mechanism transparent, commonly including generalized linear models, decision trees, sparse linear models, and rule-based classifiers. Logistic regression and linear models offer additive structure and straightforward coefficient interpretation; shallow decision trees provide explicit decision paths that can be inspected and audited. More specialized rule learners include Bayesian Rule Lists (Letham et al., 2015) and constraint-based rule sets (e.g., CORELS (Angelino et al., 2018)), which produce compact if-then structures with probabilistic or combinatorial learning procedures. These approaches provide important baselines for interpretability and can be audited post hoc, but they often remain misaligned with bedside execution requirements: even sparse models may depend on dense feature sets, require preprocessing pipelines, or produce real-valued computations that are not manually executable. Moreover, many interpretable ML methods optimize within model classes (linear scores, trees, rule lists) that do not directly correspond to guideline-style checklist workflows, and thus may improve transparency without delivering *deployability* (Rudin, 2019; Molnar et al., 2022).

Post-hoc explanations and their limitations. Similarly, post-hoc explanation methods (e.g., SHAP, LIME) can provide useful diagnostic insight into individual predictions, but they do not constrain model behavior or guarantee stability under distribution shift (Ribeiro et al., 2016; Lundberg & Lee, 2017; Adebayo et al., 2018). More fundamentally, post-hoc explanations can be faithful only locally, can vary across equivalent representations, and may give a false sense of transparency when the underlying decision boundary remains complex (Lipton, 2018; Rudin, 2019). For guideline deployment, the central requirement is not merely that a prediction can be explained, but that the decision procedure is itself simple, auditable, and reliably executable under real-world constraints.

Symbolic regression and rule learning. Symbolic regression and equation discovery methods learn structured mathematical expressions from data, including frameworks such as SINDy (Brunton et al., 2016) and modern genetic-programming systems (e.g., PySR) (Cranmer, 2023). These methods aim to recover compact functional forms with scientific interpretability and have been successful in low-dimensional dynamical systems discovery. However, their objectives and constraints typically differ from clinical score design: they target continuous functional relationships rather than discrete, actionable decision rules, and they can exhibit instability in high-dimensional, noisy, and heavily confounded observational data. More broadly, black-box time-series models (including neural ODE variants and deep sequence models) can capture rich temporal structure but are rarely compatible with bedside execution and often require substantial computational infrastructure, making them poor substitutes for guideline-style scoring systems when the deployment target is a human-executable protocol (Chen et al., 2018). Our work is complementary: we borrow the idea of structured hypothesis classes, but we focus on a constrained, checklist-oriented rule language that is explicitly aligned with clinical workflows.

Large Language Models in Clinical Applications. A rapidly growing literature studies LLMs for clinical documentation (note/discharge summary drafting), information extraction, triage and diagnostic suggestion, and medical question answering (Singhal et al., 2023; Pal et al., 2022). While these results indicate substantial medical knowledge and reasoning capacity, multiple studies emphasize that benchmark accuracy alone is insufficient for autonomous clinical decision-making: LLMs can hallucinate, exhibit instruction and context-order sensitivity, and remain difficult to calibrate and integrate into real workflows, with additional constraints from privacy and governance when patient data must be transmitted to external services (Hager et al., 2024; Williams et al., 2024). AgentScore differs fundamentally from direct LLM-based prediction: the LLM is used only during development as a constrained proposal mechanism to explore a semantic rule space, while all acceptance is determined by deterministic, data-grounded verification (and a conservative eliminative plausibility filter). The deployed artifact is a static, deterministic unit-weighted checklist that requires no LLM at inference time, avoiding the latency, cost, and reliability risks of bedside LLM invocation and ensuring that final decisions are induced by validated rules on data rather than free-form model generation.

C.3. Clinical model deployment and workflow integration

Deployment challenges in clinical ML. A recurring theme in clinical machine learning is the gap between retrospective performance and real-world impact. Predictors trained on EHR data can fail under dataset shift, evolving clinical practice, missingness, and changes in coding or documentation. Practical deployment further requires robust integration into clinical workflows, governance, monitoring, and often regulatory review, all of which impose constraints beyond standard ML benchmarks. These challenges are widely documented and have motivated calls for rigorous evaluation, transparent reporting, and human-centered design in clinical decision support (Goldstein et al., 2016; Kelly et al., 2019; Hofer et al., 2020).

Models aligned with guideline workflows. A promising direction is to align model outputs with existing clinical decision points rather than attempting to replace workflows end-to-end. In several domains, ML systems act as perception or measurement enhancers (e.g., image-based classification in dermatology, computational pathology, or radiology) (Kather et al., 2020; Esteva et al., 2017; Cao et al., 2023), while the downstream decision logic remains anchored in established clinical pathways and guidelines. This separation between *measurement* and *decision* can improve adoption: the model augments an upstream signal, and clinicians retain control over guideline-aligned thresholds and actions. This paradigm suggests that the most deployable ML systems may be those that explicitly target the model classes and interfaces used in routine practice.

Interpretability versus deployability. Finally, it is important to distinguish interpretability from deployability. Interpretability concerns whether humans can understand the rationale for a model’s outputs; deployability concerns whether the model can be executed reliably within the operational constraints of the target setting. A model can be interpretable yet non-deployable if it requires non-routine inputs, complex computations, or specialized infrastructure; conversely, a deployable guideline score may be less expressive yet succeed because it is auditable, memorable, and tightly coupled to actionable thresholds. This distinction motivates constraining the hypothesis class to *guideline-compatible* forms rather than optimizing flexible predictors and attempting to explain or simplify them post hoc (Rudin, 2019). AgentScore operationalizes this principle by searching over a clinically motivated rule language while enforcing hard structural constraints that ensure the learned artifact is executable at the bedside. This distinction is increasingly reflected in clinical AI reporting guidance, which separates transparency of model internals from suitability for real-world execution (Moons et al., 2025).

In summary, prior approaches are typically either deployable but manually designed (e.g., CURB-65), or data-driven but not checklist-deployable and not generative over semantic rules (e.g., regression-to-points, RiskSLIM/FasterRisk, trees), whereas AgentScore is both deployable-by-design and learns the rules themselves (see Table 7).

Table 7. **At-a-glance comparison.** Interpretable vs. deployable vs. rule-generation capability, with representative examples.

Approach	Interpretable	Checklist-deployable	Generates rules	Example
Expert design	✓	✓	✓ (manual)	CURB-65
Regression + rounding	✓	partial	✗	Framingham
RiskSLIM / FasterRisk	✓	partial	✗	—
Decision trees	✓	✗	✗	CART
AgentScore	✓	✓	✓ (automated)	This work

D. Experimental details

D.1. Datasets

We evaluate AgentScore on ten prediction tasks spanning five data sources:

1. **MIMIC-IV** (v3.1) (Johnson et al., 2023): A de-identified electronic health record (EHR) database from Beth Israel Deaconess Medical Center containing over 400,000 hospital admissions.
2. **eICU Collaborative Research Database** (v2.0) (Pollard et al., 2018): A multicenter critical care database comprising ICU stays from 208 hospitals across the United States.

3. **UK Cystic Fibrosis (CF) Registry**: A national registry containing annual longitudinal follow-up records for individuals with cystic fibrosis in the United Kingdom.
4. **Canadian Cystic Fibrosis Registry**: A national population-based registry used for external validation of CF mortality prediction.
5. **PhysioNet Challenge 2012** (Silva et al., 2012): A publicly available ICU mortality benchmark comprising 8,000 patient episodes from two hospitals.

Task definitions. Table 8 summarizes outcome definitions, prediction horizons, index times, and inclusion criteria. We provide additional clarifications below to ensure precise reproducibility.

Observation windows. For all time-series tasks, only measurements recorded strictly *before* the prediction horizon are used to prevent information leakage:

- MIMIC AF, HF, AKI, COPD, pneumonia (lung), lung cancer (cancer), and ICU mortality tasks use laboratory and vital-sign measurements up to **245 hours** from hospital admission or ICU intime.
- MIMIC length-of-stay tasks use measurements from the **first 24 hours** only.
- eICU tasks use measurements from the **first 6 hours** of ICU admission.

Outcome construction. Mortality outcomes correspond to binary in-hospital death unless otherwise specified. Length-of-stay (LOS) outcomes are defined using clinically meaningful thresholds: ICU LOS >3 days; LOS >5 days for COPD and lung cancer; and LOS >7 days for pneumonia. For cystic fibrosis cohorts, the outcome is defined as death within a fixed prediction horizon following the index annual visit.

Missing data handling. Time-series variables are imputed using forward fill; if no prior measurement exists within the observation window, backward fill is applied when later measurements are available. For baselines that do not operate on temporal data, the final observed value per variable is used with median imputation. For AgentScore, if a required input is missing at prediction time, the rule evaluates to false.

Table 8. Task definitions. Outcome definitions, prediction horizons, index times, and key inclusion criteria for each prediction task.

Task	Outcome	Horizon	Index Time	Inclusion Criteria
MIMIC-AF	In-hospital mortality	Stay	Admission	Adults with AF (ICD-9: 42731; ICD-10: I48.*)
MIMIC-HF	In-hospital mortality	Stay	Admission	Adults with heart failure (ICD-9: 428.*; ICD-10: I50.*)
MIMIC-AKI	AKI development	Stay	Admission	Adults; AKI per ICD-9: 584.* or ICD-10: N17.*
MIMIC-COPD	LOS >5 days	Stay	Admission	Adults with COPD (ICD-9: 491.*, 492.*, 496; ICD-10: J43.*, J44.*)
MIMIC-Lung	LOS >7 days	Stay	Admission	Adults with pneumonia (ICD-9: 480–486; ICD-10: J12–J18)
MIMIC-Cancer	LOS >5 days	Stay	Admission	Adults with lung cancer (ICD-9: 162; ICD-10: C34.*)
eICU-Vaso	Vasopressor initiation	Delayed	ICU admission	Adults; excludes stays <1h
eICU-LOS	ICU LOS >3 days	Stay	ICU admission	Adults; excludes stays <1h
CF-UK	Mortality	3 years	Annual visit	Patients with annual follow-up records
CF-CA	Mortality	Horizon-based	Annual visit	Patients with ≥ 2 annual records
ICU-Mort.	In-hospital mortality	Stay	ICU admission	PhysioNet 2012 cohort

Train/validation/test splits. We use 5-fold stratified cross-validation over trajectories (hospital admissions or ICU stays). Stratification preserves outcome prevalence across folds, and all splits are deterministic with a fixed random seed. For the CF cohort comparison, models are trained on the UK CF Registry and externally validated on the Canadian CF Registry to assess cross-population generalization. For ICU mortality external validation, models are trained on hospital A and evaluated on hospital B. Because fold-level splits are unavailable in this setting, results are aggregated over five independent random training seeds. For AgentScore, the training portion of each fold is further split into 80% used for rule construction and 20% used for internal validation during score selection.

Statistical analysis. We evaluate predictive performance using AUROC. For AgentScore, predicted probabilities are computed as

$$\hat{p} = \frac{\text{count}}{n_{\text{rules}}},$$

where *count* denotes the number of satisfied rules. Statistical significance is assessed using paired tests across cross-validation folds, including both a paired t-test and a Wilcoxon signed-rank test. One-sided alternatives are used with hypothesis H_1 : AgentScore > baseline. In some folds, heavily regularized or discretized baselines fail to produce a non-degenerate predictor (e.g., all coefficients collapse to zero). In these cases, AUROC is conservatively set to 0.5 to enable paired comparisons without discarding folds.

Table 9. **Dataset summary statistics.** Patients denote unique individuals; observations denote total time-indexed records.

Statistic	MIMIC AF	eICU Vaso	eICU LOS	MIMIC HF	MIMIC Lung	MIMIC Cancer	MIMIC COPD	MIMIC AKI	CF-CA	CF-UK	ICU-Mort.
Patients	79,779	195,339	195,339	80,611	29,180	8,245	44,246	546,028	7,582	11,741	8,000
Features	74	60	60	74	74	74	74	75	107	132	42
Observations	8.5M	195K	195K	9.2M	451K	114K	614K	38.3M	144K	58.7K	381K
Pos. (%)	5.4	10.7	25.3	5.0	46.2	44.6	42.0	13.4	32.0	4.9	14.0

Feature binarization. Score-learning methods (RiskSLIM, FasterRisk, and PLR variants) require binary indicator features to learn integer-valued scoring systems (Liu et al., 2022). For each continuous variable $x_{\cdot, j}$, we construct a set of binary threshold indicators $\tilde{x}_{\cdot, j, \theta} = \mathbb{I}[x_{\cdot, j} \leq \theta]$. When the number of unique values in column j is small, we use all unique values as thresholds (excluding the maximum to avoid constant predictors). When the number of unique values exceeds a configurable cap (default: 1000), we instead use quantile-based thresholds at probabilities $\{1/q, 2/q, \dots, (q-1)/q\}$ for $q = 1000$ to maintain computational tractability. Constant dummy columns (all zeros or all ones on the training set) are dropped. This *threshold-dummy transform* is fitted on training data and applied identically to test data to prevent leakage.

D.2. Baselines

We note that none of the existing score-learning or interpretable modeling approaches natively support the construction of unit-weighted N -of- M clinical checklists as produced by AgentScore. Methods such as RiskSLIM, FasterRisk, and pooled piecewise-linear rule (PLR) variants optimize over sparse linear models with integer or real-valued coefficients, but do not enforce unit weights or checklist-style aggregation. AutoScore can generate integer-valued point systems, but the resulting scores are not bounded and may assign large cumulative point totals, which complicates memorability and bedside use in practice.

To ensure a fair and meaningful comparison, we restrict all integer-based baselines to the coefficient set $\{-1, 0, +1\}$ and limit model sparsity to match the maximum number of rules used by AgentScore. This aligns the hypothesis classes as closely as possible while preserving each method’s native optimization procedure.

Small integer-based score-learning baselines. We compare against established methods for learning sparse, interpretable scoring systems:

- **RiskSLIM** (Ustun & Rudin, 2015): A mixed-integer programming (MIP) approach for learning sparse linear models with integer coefficients. We use the CPLEX solver with a maximum runtime of 3000 seconds and an L_0 penalty $c_0 = 10^{-6}$. Features are standardized to zero mean and unit variance, and the threshold-dummy transform is optionally applied. Coefficients are constrained to $\{-1, 0, +1\}$, and the sparsity budget is matched to AgentScore.
- **FasterRisk** (Liu et al., 2022): A fast coordinate-descent-based algorithm for learning sparse risk scores. We use the official Python implementation with sparsity constraint $k = 6$ and coefficient bounds $\{-1, 0, +1\}$. Features are standardized prior to fitting, and the threshold-dummy transform is optionally applied via configuration.

AutoScore. AutoScore (Xie et al., 2020) is a framework for automatically constructing point-based clinical scores. We use the reference R implementation with random forest-based feature selection (100 trees), equal-frequency discretization into four bins for continuous variables, and a maximum score of 100 points. AutoScore performs its own internal binning and does not rely on the shared threshold-dummy transform. While AutoScore produces integer-valued scores, the resulting point totals are not bounded to unit weights, leading to less compact and less checklist-like models.

Linear and tree-based baselines. We include standard interpretable machine-learning comparators operating on continuous features without binarization. Logistic regression is trained with feature standardization (zero mean, unit variance), median imputation for missing values, and the SAGA optimizer with a maximum of 2000 iterations. As a non-linear but still interpretable comparator, we include a CART decision tree with maximum depth four and a minimum of 20 samples per leaf.

PLR baselines. Following Liu et al. (2022), we include pooled piecewise-linear rule (PLR) baselines, which expand continuous variables into collections of binary threshold indicators prior to fitting sparse linear models. This expansion uses the same threshold-dummy transform applied to other baselines.

Each PLR model is trained by solving an ElasticNet-regularized logistic regression problem over the expanded feature space, with mixing parameter $\alpha \in \{0, 0.1, \dots, 1.0\}$ and regularization strength $C \in [10^{-4}, 10^2]$ on a logarithmic scale, yielding real-valued coefficients.

To obtain integer-valued scoring systems, we apply the rounding procedures introduced by Ustun & Rudin (2019), which convert real-valued PLR solutions into discrete coefficients in $\{-1, 0, +1\}$. For each dataset, we generate a pool of approximately 1,100 candidate PLR models (11α values \times 8 regularization settings \times multiple random seeds) and apply multiple rounding strategies. The final model is selected as the rounded solution with the lowest logistic loss.

Specifically, we consider:

- *PLR-RD*: Direct rounding after truncating coefficients to $[-1, +1]$.
- *PLR-RDU*: Unit-weighted rounding (Burgess method), assigning coefficients based solely on sign.
- *PLR-RSD*: Rescaling coefficients to unit magnitude prior to rounding.
- *PLR-Rand*: Randomized rounding based on fractional coefficient values.
- *PLR-RDP*: Sequential, loss-aware rounding that locally minimizes logistic loss.
- *PLR-RDSP*: Sequential rounding followed by discrete coordinate descent (25 iterations) to further reduce loss.

D.3. AgentScore Hyperparameters

Table 10 summarizes the hyperparameters used for AgentScore across all experiments.

We set `auc_threshold`= 0.60 empirically as the lowest univariate AUROC that still justifies including a rule under a sparse rule budget. For diversification, `jaccard_threshold`= 0.9 filters near-duplicate rules (high overlap in covered positives); we allow an exception when a candidate improves AUROC by at least 0.01 over the incumbent. For scoring, we use a deterministic Youden- J thresholding objective by default, but other objectives (e.g., prioritizing sensitivity or PPV) can be substituted depending on the desired operating point.

Table 10. AgentScore hyperparameters. Default values used across all experiments unless otherwise specified.

Parameter	Value	Description
<i>Feature Agent</i>		
<code>max_rules</code>	6	Maximum number of rules in final score
<code>iterations</code>	100	Number of LLM proposal iterations
<code>auc_threshold</code>	0.60	Minimum univariate AUROC to retain a candidate rule
<code>temperature</code>	1.0	LLM sampling temperature for diversity
<code>logic_depth</code>	1	Maximum logical composition depth (atomic single-condition rules)
<i>Score Diversification</i>		
<code>jaccard_threshold</code>	0.9	Maximum Jaccard similarity on positive cases
<code>min_pos_gain</code>	0.01	Minimum AUROC gain to accept a similar rule
<i>Scoring Agent</i>		
<code>refine_steps</code>	10	Number of refinement iterations
<code>objective</code>	Youden	Threshold selection objective (Youden's J)

D.4. Compute resources

Experiments were conducted on a shared Linux workstation with dual AMD EPYC 7713 CPUs (128 physical cores), 1 TB of system memory, and a single NVIDIA RTX 6000 Ada GPU (48 GB VRAM), using CUDA 11.5. We use GPT-5 (version 2025-08-07), GPT-4o (version 2024-11-20) and Deepseek V3.2 (version 2026-05-01-preview) via API calls as provided on Microsoft Azure.

E. Extended results

E.1. Formal Optimization Landscape and Complexity

Problem Formulation. Let $\mathcal{D} = \{(x_i, y_i)\}_{i=1}^N$ be a dataset where $x_i \in \mathbb{R}^d$ and $y_i \in \{0, 1\}$. We define a rule grammar \mathcal{G} generating a universe of logical predicates $\mathcal{R}_{\text{univ}}$. The objective is to select a subset $S \subset \mathcal{R}_{\text{univ}}$ to form a unit-weighted score $f_S(x) = \sum_{r \in S} r(x)$ that maximizes a utility metric \mathcal{J} .

$$\max_{w \in \{0,1\}^{|\mathcal{R}_{\text{univ}}|}, k \in \mathbb{Z}} \mathcal{J}(w, k; \mathcal{D}) \quad \text{s.t.} \quad \|w\|_0 \leq M_{\max}, \quad \hat{y} = \mathbb{I}\left(\sum_j w_j r_j(x) \geq k\right). \quad (2)$$

Here \mathcal{J} is a utility metric (e.g., AUROC) and $\|w\|_0$ is the ℓ_0 pseudo-norm.

Why Standard Solvers Fail.

1. **The “Generation–Selection” Gap:** State-of-the-art interpretable solvers such as RiskSLIM and FasterRisk act as *selectors*, requiring a pre-computed feature matrix $X \in \{0, 1\}^{N \times |\mathcal{R}_{\text{univ}}|}$. They cannot generate semantic rules dynamically; any clinically meaningful derived constructs (ratios, trends, shallow logic) must be manually engineered and materialized as columns *a priori*.
2. **Failure of Continuous Relaxation (e.g., Lasso):** Relaxing $w \in \{0, 1\}^{|\mathcal{R}_{\text{univ}}|}$ to continuous weights $w \in \mathbb{R}^{|\mathcal{R}_{\text{univ}}|}$ introduces a substantial **integrality gap**: continuous relaxations induce fractional solutions, and rounding them can change the induced decision boundary and utility relative to the discrete optimum. In checklist learning, where both the score and the operating threshold are discrete, such rounding effects are often amplified.
3. **Failure of Classical Heuristics (Genetic Algorithms, SA):** Standard heuristic searches struggle with the semantic structure of the rule space:
 - *Undefined Metric Space:* Crossover operators in Genetic Algorithms require a meaningful metric space. It is unclear how to interpolate between “Age > 65” and “Lactate < 2.0”.
 - *Sparse Fitness Landscape:* A random mutation to a complex rule (e.g., changing a temporal window from 24h to 1h) often yields a rule with AUROC ≈ 0.5 . Without semantic guidance, random search (and simulated annealing) wastes the large majority of evaluations on statistically irrelevant candidates.

Combinatorial and Physical Intractability (order-of-magnitude). The necessity of AgentScore is driven by the sheer scale of the grammar-induced search space. Below we provide an *order-of-magnitude* breakdown of the candidate space size for a representative clinical task ($p = 50$ variables, $N = 5 \times 10^5$ patients). For clarity, we omit several additional rule families (e.g., some higher-arity compositions and additional temporal operators); including them would only increase the space further.

1. *Primitive Rules:* With $T = 20$ quantile thresholds and range constraints, a crude count gives

$$|\mathcal{R}_{\text{prim}}| \approx p \times (2T + T^2) \approx 50 \times 440 \approx 2.2 \times 10^4.$$

2. *Compositional Rules:* Allowing depth-1 logical operators (AND/OR) between pairs of primitives yields, up to constants,

$$|\mathcal{R}_{\text{comp}}| \approx 2 \cdot \binom{|\mathcal{R}_{\text{prim}}|}{2} \approx \mathcal{O}(|\mathcal{R}_{\text{prim}}|^2) \approx (2.2 \times 10^4)^2 \approx 4.8 \times 10^8.$$

3. Additional Variants (Temporal + Ratios): Introducing simple temporal summaries (e.g., $W = 4$ windows $\times 3$ stats = 12 variants) and a restricted set of arithmetic ratios/differences over variable pairs ($\binom{50}{2} \approx 1225$) increases the candidate universe by large multiplicative factors. An order-of-magnitude approximation is

$$|\mathcal{R}_{\text{univ}}| \approx |\mathcal{R}_{\text{comp}}| \times (1 + 12_{\text{temporal}}) \times (1 + 1225_{\text{ratios}}) \approx (4.8 \times 10^8) \times 13 \times 1226 \approx 7.6 \times 10^{12}.$$

The Physical Barriers. *The Memory Wall:* Instantiating a full binary feature matrix $X \in \{0, 1\}^{N \times |\mathcal{R}_{\text{univ}}|}$ for matrix-based solvers would require storing on the order of

$$N \times |\mathcal{R}_{\text{univ}}| \approx (5 \times 10^5) \times (7.6 \times 10^{12}) \approx 3.8 \times 10^{18}$$

binary entries. Even under ideal bit-packing (1 bit per entry), this is

$$3.8 \times 10^{18} \text{ bits} \approx 4.75 \times 10^{17} \text{ bytes} \approx 475 \text{ PB}.$$

In practice, sparse/dense representations and metadata overhead would increase this further. This creates a hard physical constraint: the full rule matrix cannot be pre-computed; features must be generated on-the-fly.

The Time Wall: Even with on-the-fly generation, assuming a realistic evaluation time of $\tau = 0.1$ s per rule (including temporal feature extraction over $N = 5 \times 10^5$ patients),

$$\text{Time} \approx |\mathcal{R}_{\text{univ}}| \times \tau \approx 7.6 \times 10^{12} \times 0.1\text{s} = 7.6 \times 10^{11}\text{s} \approx 24,000 \text{ years}.$$

Conclusion. The problem space is too large for enumeration (Time Wall), too large for standard matrix-based solvers (Memory Wall), and ill-suited for gradient-based or random heuristics (integrality and semantic gaps). This motivates AgentScore: using an LLM to learn a proposal distribution $P_\theta(r)$ that navigates the semantic structure of the rule space, alleviating the “cold start” problem of finding high-utility rules in a sparse combinatorial landscape.

E.2. Effect of different LLM backbones

AgentScore relies on a language model to navigate the rule space by proposing semantically plausible candidates. While the downstream evaluation, acceptance, and selection procedures are fully deterministic, the quality of the proposal distribution depends on the underlying LLM. We therefore assess the sensitivity of AgentScore to the choice of language model backbone. For the main experiments, we use GPT-5, a frontier closed-source model. To evaluate robustness to model choice, cost, and openness, we additionally consider a strong open-source alternative (DeepSeek V3.2) as well as a computationally cheaper proprietary model (GPT-4o).

Across all datasets, GPT-5 yields the strongest overall performance, however, the performance gap to GPT-4o and DeepSeek V3.2 is small, with all models achieving competitive average AUROC (Figure 4). These results highlight two practical implications. First, the framework remains effective under substantially lower-cost or open-source model choices, improving accessibility and reproducibility. Second, because the LLM is used solely as a proposal mechanism and never bypasses deterministic statistical validation, the overall system is expected to improve monotonically as language models advance. Future gains in LLM reasoning quality are therefore likely to translate directly into more efficient search and higher-quality guideline-style scoring systems, without requiring changes to the underlying optimization framework.

E.3. Risk calibration and score monotonicity

For clinical deployment, performance metrics such as AUROC are necessary but not sufficient. In practice, clinicians do not treat scoring systems as purely binary classifiers. Instead, scores are used to *contextualize risk*: borderline scores may prompt individualized clinical judgment, while very high scores often trigger heightened vigilance, escalation, or additional review even when the clinician’s prior concern is low. Consequently, a clinically usable scoring system must exhibit *risk monotonicity*, such that higher scores correspond to systematically higher event rates.

To assess this property, we analyze outcome prevalence as a function of the discrete score value produced by AgentScore. Across all datasets, we observe a consistent and approximately monotonic increase in empirical risk with increasing score (Figure 5). This indicates that the learned unit-weighted checklists preserve ordinal risk structure and support meaningful risk stratification beyond a single operating threshold.

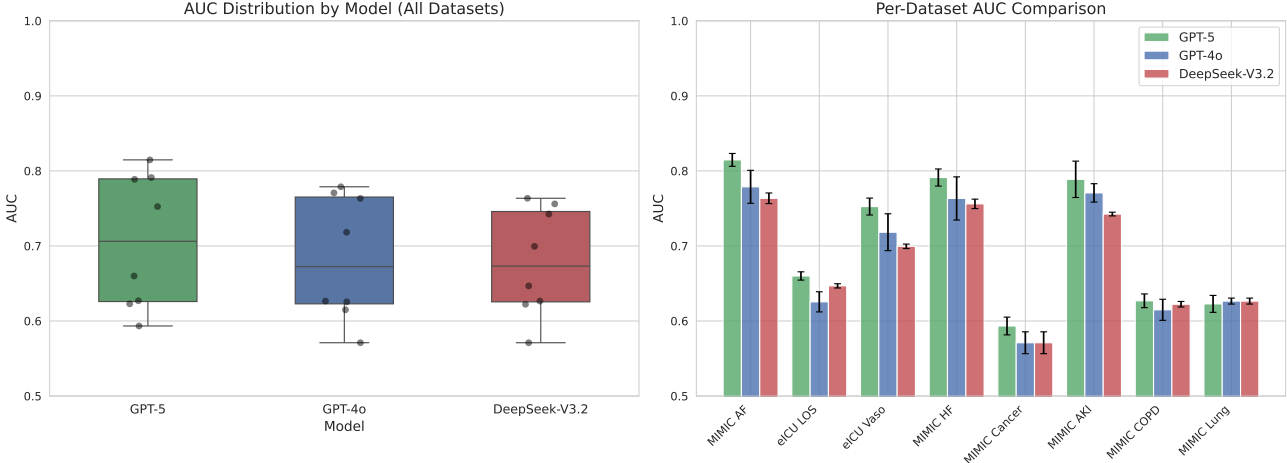


Figure 4. Effect of LLM backbone choice. Performance of AgentScore across different language-model backbones. While GPT-5 attains the strongest results on average, GPT-4o and DeepSeek V3.2 exhibit comparable performance trends, suggesting limited sensitivity to the specific LLM used for rule proposal.

The only apparent deviation from strict monotonicity occurs in the MIMIC Lung dataset, where the score bin of zero exhibits a slightly higher positive rate than the score bin of one. This effect is attributable to extreme data sparsity: only 13 patients fall into the zero-score bin, compared to several thousand patients in all other bins. When accounting for sampling variability, the overall risk trend remains monotone.

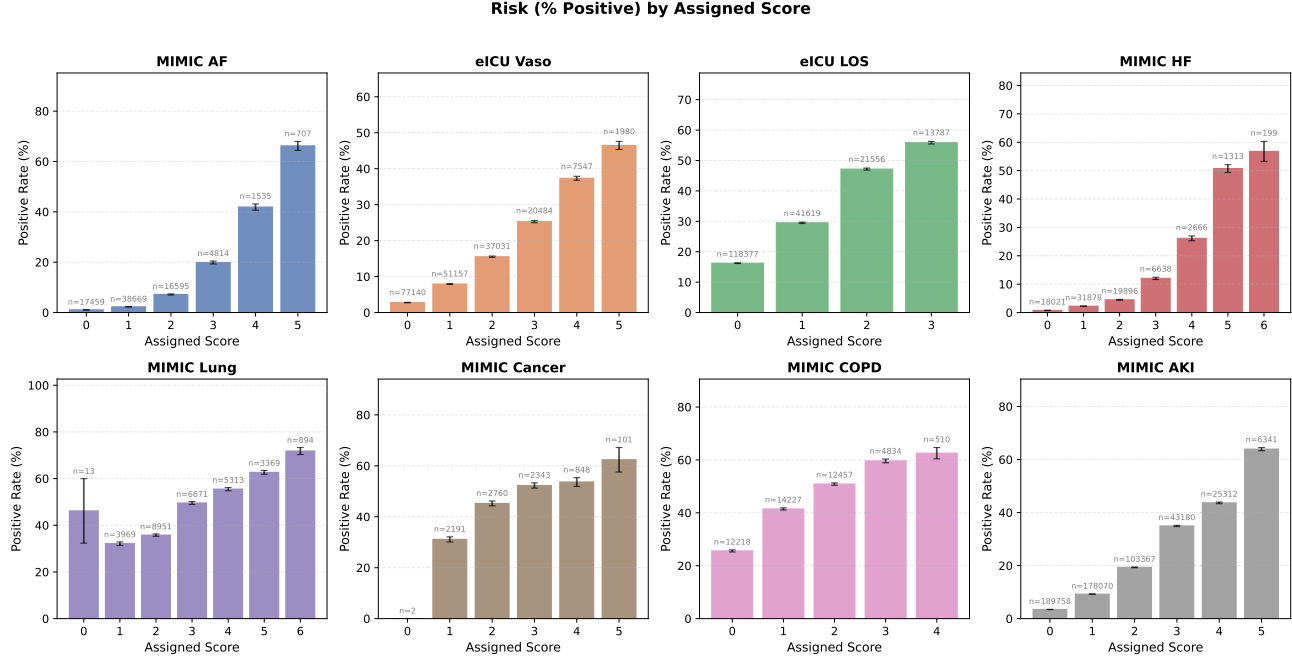


Figure 5. Risk monotonicity across score values. Empirical outcome prevalence (percentage positive) as a function of the discrete AgentScore value.

E.4. Effect of guideline size

Throughout the paper, we restrict the maximum number of rules to $M_{\max} = 6$, reflecting a conservative upper bound for checklists that remain easily memorizable and executable at the bedside while achieving competitive predictive performance. In practice, however, clinical stakeholders may prefer even smaller scores, motivating an explicit trade-off between model

complexity and accuracy.

To characterize this trade-off, we vary the maximum allowed number of rules and evaluate predictive performance as a function of checklist size. Across all datasets, performance increases smoothly and predictably with the number of included rules (Figure 6), yielding a clear accuracy–complexity Pareto frontier. Notably, in many tasks, strong performance is already achieved with only four or five rules, with diminishing returns beyond this point.

These results provide clinicians and guideline developers with direct control over deployability: additional rules can be retained when modest gains in accuracy are clinically meaningful, or omitted to maximize simplicity, memorability, and ease of use. This flexibility highlights the practical advantage of learning within a strictly constrained, unit-weighted checklist model class.

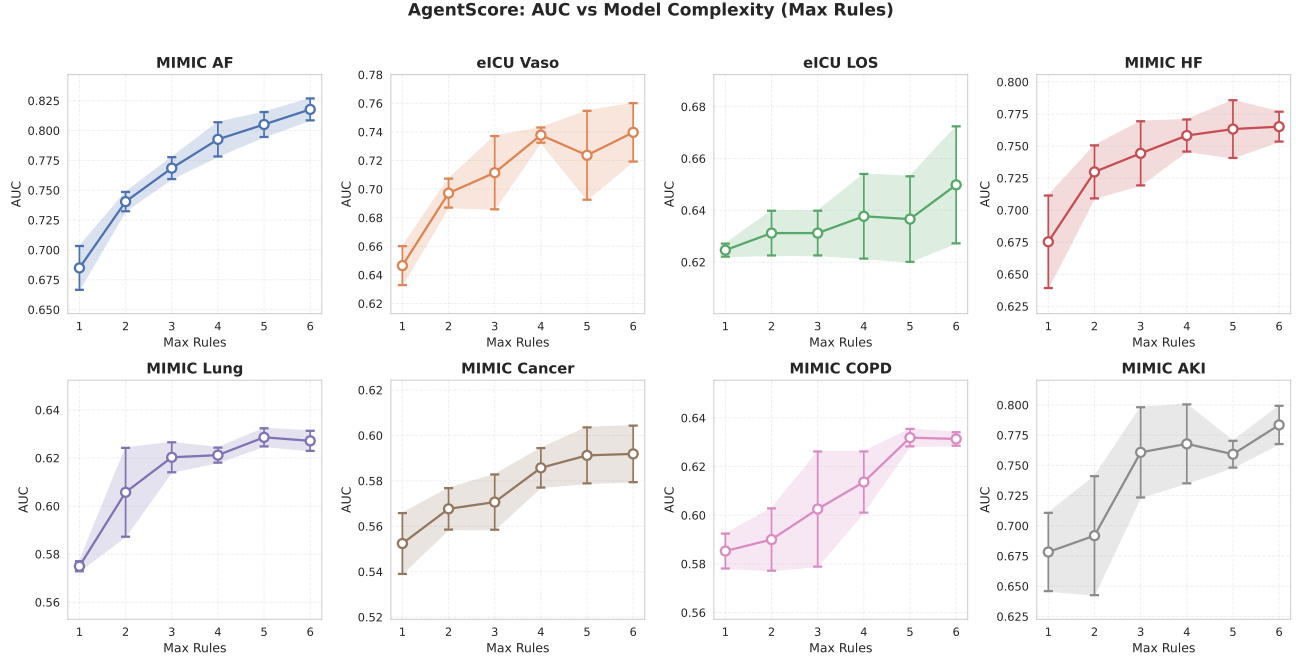


Figure 6. Accuracy–complexity trade-off. AUROC as a function of the maximum number of rules allowed in the checklist. Performance improves monotonically with rule set size, illustrating a clear deployability–accuracy Pareto frontier.

Statistical analysis. We evaluate predictive performance using AUROC. For AgentScore, predicted probabilities are computed as

$$\hat{p} = \frac{\text{count}}{n_{\text{rules}}},$$

where *count* denotes the number of satisfied rules. Statistical significance is assessed using paired tests on fold-level AUROC values across the 8 selected datasets (5 folds each; $n = 40$ paired observations per comparison), including a paired t-test and a Wilcoxon signed-rank test. Tests are two-sided, and *p*-values are corrected for multiple comparisons using Holm–Bonferroni. We additionally report bootstrap 95% confidence intervals for mean differences and Cohen’s *d* effect sizes. If a method is missing for a fold/dataset, AUROC is set to 0.5 to preserve pairing.

E.5. Scoring system analysis

We analyze the structure of the scoring systems produced by AgentScore across a full cross-validation run. Concretely, for each dataset we collect the final checklist generated in each of the five folds and summarize the distribution of rule families induced by the rule grammar (Appendix A). Figure 7 reports the resulting composition statistics, quantifying how often the learned checklists rely on different rule types, demonstrating that the framework consistently leverages multiple rule families rather than collapsing to a single template. To illustrate the learned artifacts, Table 12 presents four representative AgentScore checklists sampled. Each checklist is unit-weighted and executable as an *N*-of-*M* procedure, where the total score is the number of satisfied rules and the decision threshold *K* is selected on validation data. These

Table 11. Statistical comparison of AgentScore vs. score-based baselines. Two-sided paired tests on fold-level AUC values ($n = \text{tasks} \times 5 \text{ folds}$). p -values corrected using Holm-Bonferroni.

Baseline	n	ΔAUC	95% CI	p (t-test)	p (Wilcoxon)	Cohen's d
PLR (rd)	40	+0.109	[+0.087, +0.133]	0.000**	0.000**	+1.47
PLR (rand)	40	+0.094	[+0.073, +0.118]	0.000**	0.000**	+1.26
PLR (rdp)	40	+0.094	[+0.073, +0.118]	0.000**	0.000**	+1.26
PLR (rdsp)	40	+0.094	[+0.073, +0.118]	0.000**	0.000**	+1.26
PLR (rsrd)	40	+0.066	[+0.054, +0.079]	0.000**	0.000**	+1.67
PLR (rdu)	40	+0.058	[+0.044, +0.072]	0.000**	0.000**	+1.26
RiskSLIM	40	+0.046	[+0.033, +0.060]	0.000**	0.000**	+1.07
FasterRisk	40	+0.031	[+0.019, +0.042]	0.000**	0.000**	+0.81

examples highlight the intended output form: compact, auditable rule sets that combine simple threshold predicates with occasional shallow conjunctions and clinically interpretable derived rules (e.g., ratios), while remaining compatible with bedside execution.

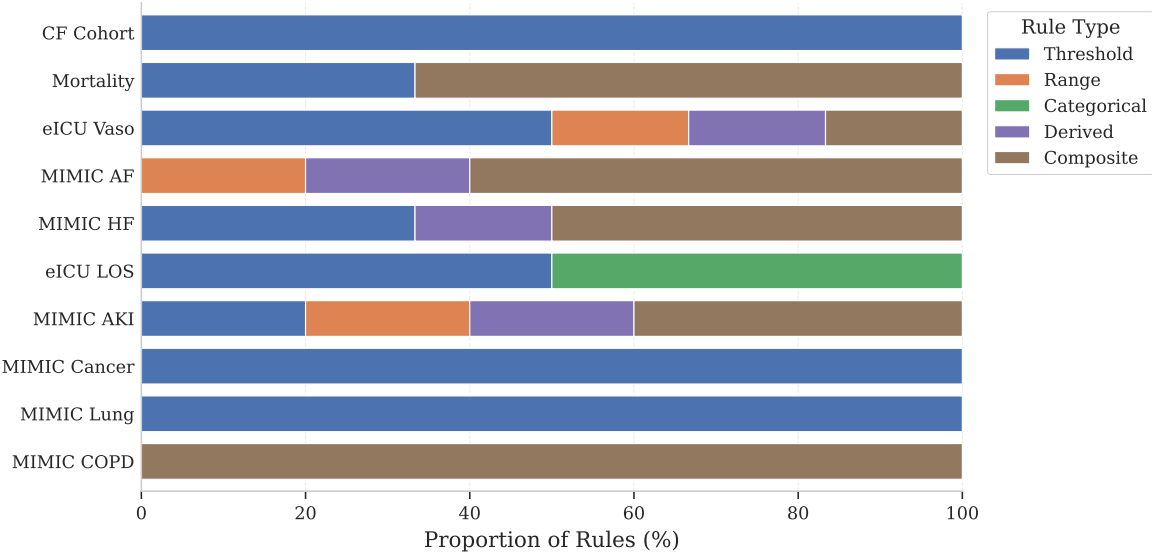


Figure 7. Rule type diversity across cross-validation. Distribution of rule families (as defined by the rule grammar) appearing in the final AgentScore checklists across five folds per dataset. Bars report the frequency with which each rule type is used, showing that learned scores draw on multiple rule families rather than collapsing to a single template.

E.6. Clinician review of scoring system deployability

We conducted a structured expert review to assess the face validity, deployability, and usability of scoring systems generated by AgentScore compared to a strong baseline. This section provides full methodological details, statistical analyses, and response distributions to complement the summary in Section 5.3.

Participants A panel of $N = 18$ practicing clinicians participated in the study. Participants were recruited from six countries across three continents and represented diverse clinical specialties. The sample was predominantly experienced: 8 participants (44.4%) reported 10+ years of clinical experience, 8 (44.4%) reported 6–10 years, and 2 (11.1%) reported 0–2 years. Overall, 89% of participants had at least 6 years of clinical experience.

Study design We employed a blinded, randomized paired-comparison design. Participants evaluated four representative scoring systems generated by AgentScore (labeled “Model B”) alongside matched outputs from FasterRisk (labeled “Model A”), a state-of-the-art integer score-learning baseline. To isolate structural and usability considerations from predictive performance, participants were explicitly instructed to assume equal discrimination and to focus exclusively on rule structure, feature choice, and bedside deployability.

Table 12. Representative AgentScore checklists (2×2 panel). Each satisfied rule contributes +1 point. The total score is the number of satisfied rules; predict positive if $S(x) \geq \tau$, where τ is selected on validation data. **Quantile thresholds.** Quantile-based cutpoints are common in clinical medicine (e.g., troponin above the 99th percentile upper reference limit; percentile-based definitions of “normal” ranges). For deployment, any quantile expression $Q_q(\cdot)$ is converted to a fixed numeric threshold estimated on a reference cohort (or precomputed and reported in guideline units); we retain the symbolic Q_q notation here to show the original rule form produced by the system.

eICU Prolonged ICU LOS (N-of-6) (Prolonged ICU Stay > 3 days Checklist)		MIMIC-IV HF Mortality (N-of-6) (HF In-Hospital Mortality N-of-M)	
Checklist rule (satisfied?)	Points	Checklist rule (satisfied?)	Points
GCS Verbal < 5	+1	$\text{HCO}_3^-/\text{Cl}^- < 0.2$	+1
GCS Eyes < 4	+1	$\text{WBC} \geq 10 \text{ and } \text{HCO}_3^- \leq 25$	+1
GCS Motor < 6	+1	$\text{BUN} \geq 30$	+1
Hematocrit < 35%	+1	$1.5 \leq \text{Cr} \leq 5.0$	+1
Heart rate ≥ 85 bpm	+1	Admission is emergency or urgent	+1
Mean BP < 65 mmHg	+1	$10 \leq \text{WBC} \leq 20$	+1
Total score	0–6	Total score	0–6
High-risk threshold	$S(x) \geq 3$	High-risk threshold	$S(x) \geq 3$
eICU Vasopressor (N-of-4) (Shock & Organ Dysfunction Checklist)		MIMIC-IV AKI (N-of-4) (Renal–Anemia–Acuity Checklist)	
Checklist rule (satisfied?)	Points	Checklist rule (satisfied?)	Points
Intubated or mechanical ventilation	+1	$\text{Cr} \geq Q_{0.75}(\text{Cr})$	+1
Heart rate / mean BP ≥ 1.5	+1	$0 \leq \text{Hematocrit} \leq 30$	+1
BUN ≥ 25 mg/dL	+1	ER admission and BUN ≥ 20	+1
$\text{WBC} \geq Q_{0.75}(\text{WBC})$	+1	$\text{BUN}/\text{Cr} \geq 20$	+1
Total score	0–4	Total score	0–4
High-risk threshold	$S(x) \geq 2$	High-risk threshold	$S(x) \geq 2$

Survey instrument The survey comprised 10 questions organized into three blocks:

Block 1: Demographics and general attitudes (Q1–Q6).

- **Q1** (Demographics): Years of clinical experience (0–2, 3–5, 6–10, 10+).
- **Q2** (5-point Likert): “I would trust a clinical scoring system generated by AI.”
- **Q3** (5-point Likert): “I would trust a clinical scoring system generated by AI *if it had been externally validated on 50,000 patients.*”
- **Q4** (5-point Likert): “Memorability is important for clinical scoring systems used at the bedside.”
- **Q5** (5-point Likert): “I would be willing to use a unit-weighted checklist (each item worth 1 point) in clinical practice.”
- **Q6** (5-point Likert): “I would be willing to use a scoring system that requires mental arithmetic (e.g., multiplying values by 2, 3, or 5) at the bedside.”

Block 2: Paired comparisons across four clinical tasks (Q7–Q9). For each of four clinical prediction tasks (ICU mortality, sepsis risk, respiratory failure, cardiac events), participants were shown two scoring systems (Model A and Model B) and asked:

- **Q7:** “Which scoring system better matches guideline-style clinical reasoning?”
- **Q8:** “Which scoring system would be easier to apply at the bedside under time pressure?”
- **Q9:** “Assuming both have been externally validated, which would you prefer to deploy?”

Block 3: Overall preference (Q10).

- **Q10:** “Overall, which scoring-system *style* would you prefer for clinical deployment?” (Model A / Model B / Neither).

Statistical analysis All analyses were pre-specified. For Likert-scale items (Q2–Q6), we report means, 95% confidence intervals, and one-sample *t*-tests against the neutral midpoint (3). For the trust comparison (Q2 vs. Q3), we used a paired *t*-test and report Cohen’s *d* as an effect size. For pairwise preference questions (Q7–Q9), we aggregated responses across the 4 clinical tasks ($n = 72$ judgments per question) and tested whether the proportion preferring Model B exceeded 50% using one-sided binomial tests; we report Cohen’s *h* as an effect size for proportions. For overall preference (Q10), we used a chi-square goodness-of-fit test against a uniform distribution and a binomial test comparing Model B to Model A (excluding “Neither” responses). All *p*-values are reported without correction for multiple comparisons; conclusions are robust to Bonferroni correction.

Trust in AI-generated scores. Baseline trust in AI-generated scores was neutral to low ($M = 2.72$, 95% CI [2.13, 3.31], $t(17) = -0.92$, $p = 0.37$). However, trust increased substantially when large-scale external validation was specified ($M = 4.39$, 95% CI [4.16, 4.62], $t(17) = 11.75$, $p < 10^{-8}$). The within-subject increase was statistically significant ($\Delta M = +1.67$, SD = 1.37; paired $t(17) = 5.15$, $p < 10^{-4}$) with a large effect size (Cohen’s *d* = 1.21).

Deployability preferences. Clinicians expressed strong willingness to use unit-weighted checklists ($M = 4.33$, 95% CI [3.91, 4.75], $t(17) = 6.23$, $p < 10^{-5}$) and moderate willingness to use scores requiring mental arithmetic ($M = 3.89$, 95% CI [3.58, 4.20], $t(17) = 5.58$, $p < 10^{-4}$). Importance of memorability was rated as neutral to high on average ($M = 3.22$, $p = 0.45$).

Pairwise comparisons. Across 72 judgments per question (18 clinicians \times 4 tasks), participants significantly preferred AgentScore (Model B) over FasterRisk (Model A) on all three dimensions:

- **Q7 (Guideline reasoning):** 85% preferred Model B (95% CI [76%, 92%]; binomial $p < 10^{-9}$, Cohen’s *h* = 0.77).
- **Q8 (Bedside ease):** 71% preferred Model B (95% CI [61%, 80%]; binomial $p < 10^{-3}$, Cohen’s *h* = 0.43).
- **Q9 (Deployment preference):** 81% preferred Model B (95% CI [71%, 89%]; binomial $p < 10^{-7}$, Cohen’s *h* = 0.66).

Within-respondent consistency. To assess reliability, we computed the proportion of respondents who gave the same answer across all four clinical tasks: 61% for Q7, 33% for Q8, and 50% for Q9. The moderate consistency for Q8 suggests that bedside-ease judgments are more task-dependent than guideline-alignment judgments.

Overall preference. When asked for their overall preferred scoring-system style for clinical deployment, 12/18 clinicians (67%) selected Model B (AgentScore), 1/18 (6%) selected Model A (FasterRisk), and 5/18 (28%) reported no preference. The distribution differed significantly from uniform ($\chi^2(2) = 10.33$, $p = 0.006$). Excluding “Neither” responses, 12/13 (92%) preferred Model B over Model A (binomial $p = 0.002$).

Qualitative observations. In free-text comments, clinicians noted that non-unit weights (e.g., +3, +5) in FasterRisk outputs would require mental arithmetic or electronic assistance, reducing reliability under time pressure. In contrast, the unit-weighted checklist structure of AgentScore was viewed as immediately executable. Participants particularly valued derived features aligned with clinical reasoning patterns (e.g., physiologic ratios such as shock index), which are standard constructs in existing guidelines but are not discoverable by fixed-feature baselines.

Limitations The sample size ($N = 18$) is modest and precludes subgroup analyses by specialty or experience level. Although participants were blinded to model identity, the structural differences between unit-weighted checklists and integer-weighted scores may have been recognizable. This study assesses face validity and usability preferences; it does not measure actual bedside performance or patient outcomes. Finally, the convenience sampling approach limits generalizability to the broader clinical population.

Summary Clinicians with substantial experience expressed strong and statistically significant preferences for AgentScore-generated unit-weighted checklists over integer-weighted baselines across guideline alignment, bedside usability, and deployment preference. Trust in AI-generated scores increased substantially when large-scale external validation was specified. These findings support the practical deployability of the scoring systems produced by AgentScore.

Clinical Evaluation of AgentScore (N=18 Clinicians)

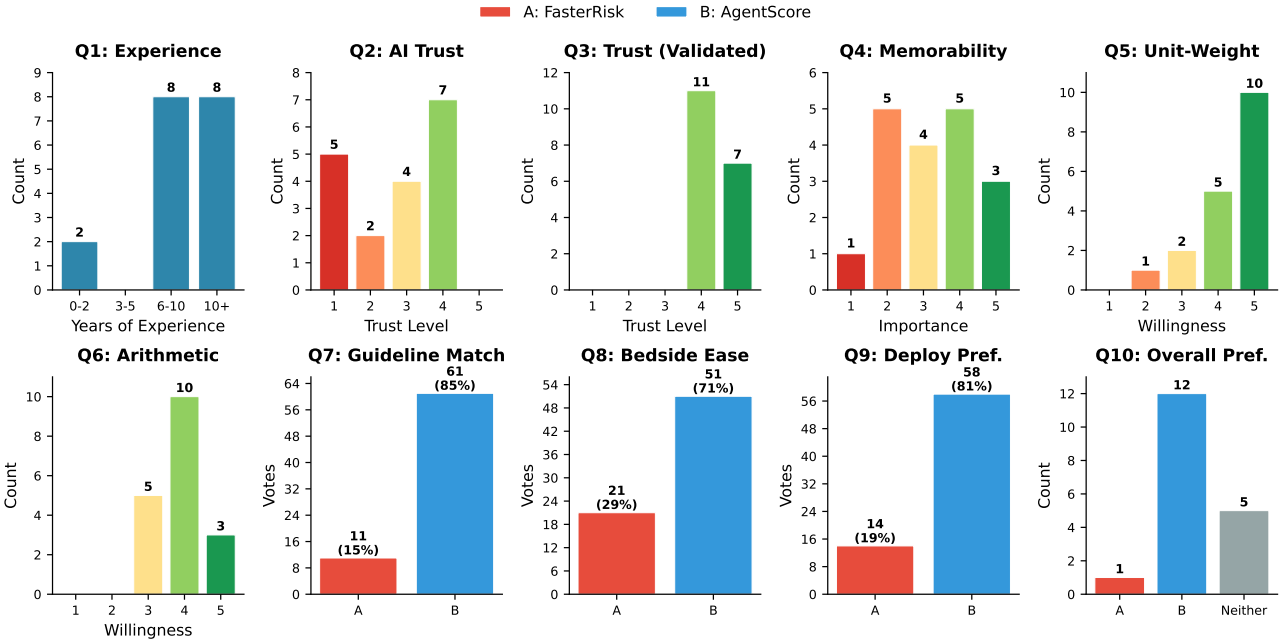


Figure 8. Clinician evaluation of scoring system deployability (N = 18). Top row: Experience distribution (Q1) and Likert-scale responses for trust (Q2–Q3) and deployability preferences (Q4–Q6). Bottom row: Aggregated pairwise preferences across 4 clinical tasks (Q7–Q9; 72 judgments each) and overall model preference (Q10). Model A: FasterRisk; Model B: AgentScore.

E.7. Wall-Clock Time

We additionally report wall-clock training time for AgentScore and all baselines. In absolute terms, AgentScore is often slower than standard baselines, primarily due to external API latency associated with language-model queries. Its runtime is nevertheless comparable to optimization-based score learning methods such as FasterRisk and RiskSLIM.

To make this cost explicit, for each cross-validation fold AgentScore issues a bounded number of language-model calls. Specifically, we perform up to 100 API calls for candidate rule generation. Each statistically valid candidate rule is then subjected to a single self-consistency check by the language model, resulting in at most an additional 100 calls. Checklist construction involves one initial guideline proposal call, followed by two refinement phases of 10 steps each, yielding at most 21 further calls. In total, the number of API calls per fold is therefore capped at approximately 220, independent of dataset size.

More importantly, training-time compute and deployment-time compute differ fundamentally across methods. For most machine-learning models, increased training complexity is typically coupled with nontrivial inference cost at test time, requiring computational infrastructure for deployment. In contrast, AgentScore incurs computational cost only during development. At deployment, inference is effectively zero-cost: the learned N -of- M unit-weighted checklist can be evaluated manually by clinicians without calculators, servers, or model execution.

Since score construction is performed offline and only once per task, differences in wall-clock training time on the order of minutes are acceptable in practice and do not affect real-world usability. These results highlight that AgentScore trades modest additional development-time compute for negligible deployment-time cost, aligning with the constraints of bedside clinical use.

F. Algorithmic Details

This section summarizes the AgentScore learning procedure and provides concise implementation details to support reproducibility. Full code will be released upon acceptance.

Table 13. Wall-clock training time per fold (seconds). All PLR variants (RD, RDU, RSRD, Rand, RDP, RDSP) share identical training time and are reported jointly.

Method	MIMIC AF	MIMIC AKI	MIMIC COPD	MIMIC HF	MIMIC CANCER	MIMIC LUNG	eICU LOS	eICU Vaso.
AgentScore	3918	4096	3594	2380	2244	3330	3145	1382
Decision Tree	2.9	6.0	1.9	3.7	0.4	1.3	3.3	3.2
Logistic	3.6	6.3	2.7	4.4	0.8	1.7	4.2	3.6
FasterRisk	1360	699	1045	1514	55.7	588	806	820
RiskSLIM	1292	193	205	1176	439	652	1934	2942
AutoScore	156	362	92	153	18.3	51.9	236	201
PLR	61	90	45.2	80	8.9	32.1	151	96

F.1. AgentScore Algorithm (High-Level)

Algorithm 1 AgentScore Framework

Require: Training data (X, y) , task description \mathcal{T} , rule budget M
Require: Validity threshold τ_{rule} , redundancy threshold δ
Ensure: Unit-weighted checklist S and decision threshold τ

Construct tool interface \mathcal{I} exposing metadata and evaluation only
Initialize rule pool $\mathcal{P} \leftarrow \emptyset$

{Phase 1: Rule Pool Generation}

while generation budget not exhausted **do**

 Propose candidate batch C from grammar \mathcal{R} using **Rule Proposal Agent**
for each proposed rule $r \in C$ **do**

 Compute AUROC(r) and overlap metrics via \mathcal{I}
if AUROC(r) $\geq \tau_{rule}$ **and** $\max_{r' \in \mathcal{P}} J_+(r, r') \leq \delta$ **then**
 $plausible \leftarrow \text{Clinical Plausibility Agent}.\text{review}(r)$
 if $plausible$ **then**
 $\mathcal{P} \leftarrow \mathcal{P} \cup \{r\}$
 end if
 end if
 end for
end while

{Phase 2: Score Construction & Refinement}

$S \leftarrow \text{Score Construction Agent}.\text{select}(\mathcal{P}, M, \mathcal{I})$
while refinement criteria not met **do**

$S \leftarrow \text{Score Construction Agent}.\text{refine}(S, \mathcal{P}, \mathcal{I})$
end while

Select final decision threshold τ on validation data
return (S, τ)

F.2. Notation, Splits, and Caching

Within each outer cross-validation fold, the training data is further split into a *construction set* \mathcal{D}_{con} and an internal *validation set* \mathcal{D}_{val} . Rule evaluation, acceptance, and redundancy filtering are performed on \mathcal{D}_{con} , while checklist selection and decision-threshold optimization are performed exclusively on \mathcal{D}_{val} . Held-out test folds are never accessed during rule generation or score construction.

We denote by $\mathcal{P} \subset \mathcal{R}$ the pool of retained candidate rules constructed during Phase 1, and by $S \subseteq \mathcal{P}$ the final checklist of size at most M assembled during Phase 2. All scores are unit-weighted by construction.

For each retained rule $r \in \mathcal{P}$, we cache its *positive-class coverage mask* on \mathcal{D}_{con} :

$$(c_r)_i = \mathbf{1}\{r(x_i) = 1 \wedge y_i = 1\}, \quad (x_i, y_i) \in \mathcal{D}_{con},$$

and write $\mathcal{C}_+ = \{c_r : r \in \mathcal{P}\}$. Redundancy is measured using the positive-class Jaccard similarity

$$J_+(r, r') = \frac{|c_r \cap c_{r'}|}{|c_r \cup c_{r'}|}, \quad r, r' \in \mathcal{P}.$$

F.3. Tool-Mediated Data Access

All interactions with the dataset are mediated by a fixed tool interface \mathcal{I} . The language model never observes raw patient-level values. Instead, it interacts exclusively through deterministic tools that expose: (i) feature names and inferred types; (ii) aggregate statistics computed on training data only (e.g., quantiles, missingness); (iii) evaluation outputs such as AUROC and coverage. No tool returns individual samples, identifiers, or free-form data.

F.4. Typed Rule Proposal and Validation

Rules are proposed as structured objects drawn from a typed grammar \mathcal{R} supporting thresholds, ranges, derived expressions, temporal summaries, and shallow logical compositions. All proposals must satisfy a strict schema; malformed rules, unknown features, or type violations are deterministically rejected prior to evaluation.

The **Clinical Plausibility Agent** functions as a binary gate applied *only after* statistical screening. It receives the symbolic rule definition and aggregate feature summaries (but no raw data) and returns a binary accept/reject decision based on clinical coherence and interpretability.

F.5. Deterministic Rule Evaluation and Retention

Each syntactically valid rule is evaluated on the construction split \mathcal{D}_{con} and retained into the rule pool \mathcal{P} if and only if it satisfies all of the following criteria: (i) its AUROC exceeds a minimum acceptance threshold τ_{rule} ; (ii) its redundancy with previously retained rules, measured by the positive-class Jaccard similarity J_+ computed over \mathcal{D}_{con} , is below a fixed threshold δ , unless the rule increases positive-class coverage by at least Δ_{\min} ; and (iii) rule-family diversity constraints are satisfied when feasible (i.e., enforcing a minimum mix across rule types such as thresholds, derived rules, and logical compositions when sufficient candidates exist; otherwise skipped).

From the pool of retained rules \mathcal{P} , a final checklist S of size at most M is assembled. The decision threshold K (predict positive if count $\geq K$) is selected on \mathcal{D}_{val} according to a specified operating objective (e.g., Youden's J , balanced accuracy, or F_1). Unless otherwise stated, we use a fixed minimum acceptance threshold of $\tau_{\text{rule}} = 0.6$ AUROC.

Computational Complexity. Conditional on a fixed stream of language-model proposals, the AgentScore pipeline is fully deterministic. All rule validation, acceptance, redundancy checks, and checklist assembly are performed via deterministic tools with no access to raw patient-level data. Let N denote the number of samples and T the total number of proposed rules. Rule evaluation scales linearly as $O(T \cdot N)$. Redundancy filtering compares each candidate against the retained pool \mathcal{P} and scales as $O(T \cdot |\mathcal{P}|)$ in the worst case. Coverage masks are stored as compact bitsets of word size w , yielding memory usage $O(|\mathcal{P}| \cdot N/w)$ for cached rule coverage, in addition to the data matrix storage. In practice, redundancy filtering dominates runtime, while memory remains modest due to bitset compression.

G. Agent prompts

This section documents the exact prompting templates used to instantiate the AgentScore framework.

Feature Proposal Prompt (AgentScore)

You are a feature selection agent for clinical risk modeling.

Task context:

`$task_description`

Propose binary (0/1) clinical features as JSON lines. All rules must follow one of the schemas below.

Allowed rule types:

```
numeric_threshold:
{"type": "numeric_threshold", "feature": str, "op": ">=" | ">" | "<=" | "<", "threshold": number}
```

```

numeric_range:
{"type":"numeric_range", "feature":str, "low":number, "high":number}

categorical_in:
{"type":"categorical_in", "feature":str, "in": [category, ...]}

binary_true:
{"type":"binary_true", "feature":str}

derived_numeric_threshold:
{"type":"derived_numeric_threshold", "expr":str, "op":">=" | ">" | "<=" | "<", "threshold":number}

count_present:
{"type":"count_present", "features": [str, ...], "min_count":int}

logical:
{"type":"logical", "op":"and" | "or", "rules": [<rule>, ...]}

percent_change:
{"type":"percent_change", "feature_t0":str, "feature_t1":str,
 "pct":number, "op":">=" | ">" | "<=" | "<", "direction":"increase" | "decrease" }

zscore_threshold:
{"type":"zscore_threshold", "feature":str, "op":">=" | ">" | "<=" | "<", "z":number}

quantile_threshold:
{"type":"quantile_threshold", "feature":str, "op":">=" | ">" | "<=" | "<", "q":float}

```

Rule diversity guidelines:

- Use a mix of rule types (thresholds, derived rules, logic).
- Include both high-value (\geq) and low-value ($<$) thresholds.
- Prefer rules that capture distinct patient subgroups.

Clinical interpretability constraints:

- Prefer features with suffixes `_last`, `_first`, `_min`, `_max`.
- Use round, clinically meaningful thresholds (e.g. $HR \geq 100$).
- Derived expressions should reflect standard clinical concepts.

Hard constraints:

- Output *only* strict JSON.
- One rule per line.
- Use only provided variable names.
- Minimum acceptable AUROC when evaluated: `auc_threshold`.

Available variables:

`$variable_list`

Aggregate analysis insights (optional):

`$analysis_context`

Tool-derived guidance (optional):

`$tool_summaries`

Suggest 1–3 candidate rules.

Clinical Plausibility Review Prompt

You are a clinical expert reviewing a proposed risk prediction rule.
Assess whether the rule is clinically plausible and meaningful.

Consider:

- Whether the direction of risk makes clinical sense.
- Whether thresholds are physiologically reasonable.
- Whether the rule is interpretable and actionable at the bedside.

Rule under review:

`$rule_json`

Respond with *only* a JSON object of the form:

```
{"plausible": true|false, "reason": "brief explanation"}
```

Score Construction Prompt (N-of-M Checklist)

You are a clinical scoring system designer.

Task context:

`$task_description`

You are given a set of binary (0/1) clinical rules.

Construct an interpretable N -of- M checklist score with the following properties:

- Each rule contributes exactly 1 point.
- The score equals the count of satisfied rules.
- Predict positive if score $\geq K$ (threshold selected automatically).
- Do not introduce new rules.

Constraints:

- Use only the provided rules.
- Maximum number of rules: `max_rules`.
- Output strict JSON with fields:
 - `name`
 - `description`
 - `rules` (list of {"rule": <rule_json>})

Candidate rules (with AUROC):

`$retained_rules_with_auc`

Return *only* the JSON specification.

Score Refinement Prompt

You are refining an existing clinical checklist score.

Current score specification:

`$current_score_json`

Evaluation metrics:

`$score_metrics`

Objective: Improve discrimination and calibration while preserving interpretability.

Constraints:

- Same schema as before.
- Maximum number of rules: `max_rules`.
- All rules are unit-weighted.
- No new rules may be introduced.

Return *only* the updated JSON specification.